LA-UR-20-24456
Approved for public release; distribution is unlimited.

Title: Re-Release of the ENDF/B VIII.0 S(,ß) Data Processed by NJOY2016

Author(s): Parsons, Donald Kent
Toccoli, Cecile A.

Intended for: Web

Issued: 2020-06-22

Re-Release of the ENDF/B VIII.0 S(α,β) Data Processed by NJOY2016

D. Kent Parsons and Cecile Toccoli
Nuclear Data Team of Group XCP-5
Los Alamos National Laboratory
LA-UR-20-nnnnn

Table of Contents

I. Introduction

"ENDF/B-VIII.0 provides a major update to the ENDF thermal scattering library. Indeed, it is nearly a completely new sub-library. Only the legacy evaluations for Al, Fe, liquid and solid methane, ortho- and para- hydrogen and deuterium and benzene and the ENDF/B-VII.1 evaluations for SiO2 are unchanged."[1,2]

Thirty four (34) materials are provided in ENDF/B-VIII.0 with a total of two hundred and fifty-three (253) evaluations. LEAPR input files are also included for each of the materials as well as "readme" files for most of the materials.

All of these 34 thermal scattering files have been re-processed with NJOY2016[3] (version 53) to produce 253 ACE files suitable for use in MCNP[4] or other similar codes. Table 1 lists the 34 materials which are included in the ENDF/B-VIII.0 thermal scattering library and also notes where major changes have occurred in the re-release.

Table 1: Listing of the TSL Materials in ENDF/B-VIII.0 (with re-release changes noted)

	ENDF/B VIII.0 tsl files	number of temperatures	Emax (eV)	ACE ID	re-release changes
1	tsl-013_Al_027.endf	6	2.277	al-27	
2	tsl-026_Fe_056.endf	6	2.277	fe-56	
3	tsl-Be-metal.endf	8	5.000001	be-met	
4	tsl-BeinBeO.endf	8	5.000001	be-beo	
5	tsl-CinSiC.endf	8	5.000001	c-sic	
6	tsl-DinD2O.endf	17	10.02133	d-d2o	
7	tsl-HinC5O2H8.endf	1	5.000001	h-luci	yes
8	tsl-HinCH2.endf	11	5.000001	h-poly	yes
9	tsl-HinH2O.endf	18	10.00008	h-lwtr	
10	tsl-HinIceIh.endf	9	5	h-ice	yes
11	tsl-HinYH2.endf	10	5	h-yh2	yes
12	tsl-HinZrH.endf	8	1.9734	h-zrh	yes
13	tsl-NinUN.endf	8	5.000001	n-un	yes
14	tsl-OinBeO.endf	8	5.000001	o-beo	
15	tsl-OinD2O.endf	17	10.02133	o-d2o	
16	tsl-OinIceIh.endf	9	5	o-ice	yes
17	tsl-OinUO2.endf	8	5.000001	o-uo2	
18	tsl-SiO2-alpha.endf	5	2.46675	sio2	yes
19	tsl-SiO2-beta.endf	2	2.46675	sio2	yes
20	tsl-SiinSiC.endf	8	5.000001	si-sic	
21	tsl-UinUN.endf	8	5.000001	u-un	
22	tsl-UinUO2.endf	8	5.000001	u-uo2	
23	tsl-YinYH2.endf	10	5	y-yh2	yes
24	tsl-ZrinZrH.endf	8	1.00022	zr-zrh	yes
25	tsl-benzene.endf	8	2	benz	

26	tsl-crystalline-graphite.endf	10	5.000001	grph	
27	tsl-l-CH4.endf	1	4.078125	lmeth	
28	tsl-ortho-D.endf	1	7.59	orthod	
29	tsl-ortho-H.endf	1	7.59	orthoh	
30	tsl-para-D.endf	1	7.59	parad	
31	tsl-para-H.endf	1	7.59	parah	
32	tsl-reactor-graphite-10P.endf	10	5.000001	grph10	yes
33	tsl-reactor-graphite-30P.endf	10	5.000001	grph30	yes
34	tsl-s-CH4.endf	1	11.385	smeth	yes

Of the 14 major changes, 10 were due to incorrect coherent elastic scattering, 2 were due to a graphite reversal, and 2 (in SiO_2) were due to incorrect processing parameters. See Section IV for details.

A few of the traditional material names have been changed from previous ACE libraries. Also notice that there are now three (3) different graphite evaluations. Crystalline graphite is the closest one to previous graphite TSL evaluations. Graphite with 10% porosity is typical for reactor usage, and graphite with 30% porosity is the most common form of graphite. These 3 forms of graphite have significantly different densities due to the porosity – say, about 2.2, 2.0, and 1.6 g/cc.

II. Details of the Re-Released S(α,β) Library

Following the long-standing nuclear data team policy of (almost) never re-using ZAID's, the ZAID's for this corrected release of S(α,β) data have been given ZAID indexes between 40 and 57. The previous release used ZAID indexes between 80 and 97. If there is a room temperature data set available, it now has a 40t suffix rather than an 80t suffix. These ZAID's are shown in Table 2.

Table 2: Listing of all 253 ACE File ZAID's and their Temperature Parameters

S(α,β)	AWR	Temp(MeV)	Temp K
al-27.40t	26.74975	2.530E-08	294
al-27.41t	26.74975	1.724E-09	20
al-27.42t	26.74975	6.894E-09	80
al-27.43t	26.74975	3.447E-08	400
al-27.44t	26.74975	5.170E-08	600
al-27.45t	26.74975	6.894E-08	800
be-beo.40t	8.93478	2.530E-08	294
be-beo.41t	8.93478	3.447E-08	400
be-beo.42t	8.93478	4.309E-08	500

be-beo.43t	8.93478	5.170E-08	600
be-beo.44t	8.93478	6.032E-08	700
be-beo.45t	8.93478	6.894E-08	800
be-beo.46t	8.93478	8.617E-08	1000
be-beo.47t	8.93478	1.034E-07	1200
be-met.40t	8.93478	2.551E-08	296
be-met.41t	8.93478	3.447E-08	400
be-met.42t	8.93478	4.309E-08	500
be-met.43t	8.93478	5.170E-08	600
be-met.44t	8.93478	6.032E-08	700
be-met.45t	8.93478	6.894E-08	800
be-met.46t	8.93478	8.617E-08	1000
be-met.47t	8.93478	1.034E-07	1200
benz.40t	0.999167	2.551E-08	296
benz.41t	0.999167	3.016E-08	350
benz.42t	0.999167	3.447E-08	400
benz.43t	0.999167	3.878E-08	450
benz.44t	0.999167	4.309E-08	500
benz.45t	0.999167	5.170E-08	600
benz.46t	0.999167	6.894E-08	800
benz.47t	0.999167	8.617E-08	1000
c-sic.40t	11.89365	2.585E-08	300
c-sic.41t	11.89365	3.447E-08	400
c-sic.42t	11.89365	4.309E-08	500
c-sic.43t	11.89365	5.170E-08	600
c-sic.44t	11.89365	6.032E-08	700
c-sic.45t	11.89365	6.894E-08	800
c-sic.46t	11.89365	8.617E-08	1000
c-sic.47t	11.89365	1.034E-07	1200
d-d2o.40t	1.9968	2.530E-08	294
d-d2o.41t	1.9968	2.444E-08	284
d-d2o.42t	1.9968	2.585E-08	300
d-d2o.43t	1.9968	2.789E-08	324
d-d2o.44t	1.9968	3.016E-08	350
d-d2o.45t	1.9968	3.220E-08	374
d-d2o.46t	1.9968	3.447E-08	400
d-d2o.47t	1.9968	3.650E-08	424
d-d2o.48t	1.9968	3.878E-08	450
d-d2o.49t	1.9968	4.081E-08	474
d-d2o.50t	1.9968	4.309E-08	500
d-d2o.51t	1.9968	4.512E-08	524
d-d2o.52t	1.9968	4.740E-08	550
d-d2o.53t	1.9968	4.943E-08	574
d-d2o.54t	1.9968	5.170E-08	600

d-d2o.55t	1.9968	5.374E-08	624
d-d2o.56t	1.9968	5.601E-08	650
fe-56.40t	55.45443	2.530E-08	294
fe-56.41t	55.45443	1.724E-09	20
fe-56.42t	55.45443	6.894E-09	80
fe-56.43t	55.45443	3.447E-08	400
fe-56.44t	55.45443	5.170E-08	600
fe-56.45t	55.45443	6.894E-08	800
grph.40t	11.89365	2.551E-08	296
grph.41t	11.89365	3.447E-08	400
grph.42t	11.89365	4.309E-08	500
grph.43t	11.89365	5.170E-08	600
grph.44t	11.89365	6.032E-08	700
grph.45t	11.89365	6.894E-08	800
grph.46t	11.89365	8.617E-08	1000
grph.47t	11.89365	1.034E-07	1200
grph.48t	11.89365	1.379E-07	1600
grph.49t	11.89365	1.723E-07	2000
grph10.40t	11.89365	2.551E-08	296
grph10.41t	11.89365	3.447E-08	400
grph10.42t	11.89365	4.309E-08	500
grph10.43t	11.89365	5.170E-08	600
grph10.44t	11.89365	6.032E-08	700
grph10.45t	11.89365	6.894E-08	800
grph10.46t	11.89365	8.617E-08	1000
grph10.47t	11.89365	1.034E-07	1200
grph10.48t	11.89365	1.379E-07	1600
grph10.49t	11.89365	1.723E-07	2000
grph30.40t	11.89365	2.551E-08	296
grph30.41t	11.89365	3.447E-08	400
grph30.42t	11.89365	4.309E-08	500
grph30.43t	11.89365	5.170E-08	600
grph30.44t	11.89365	6.032E-08	700
grph30.45t	11.89365	6.894E-08	800
grph30.46t	11.89365	8.617E-08	1000
grph30.47t	11.89365	1.034E-07	1200
grph30.48t	11.89365	1.379E-07	1600
grph30.49t	11.89365	1.723E-07	2000
h-h2o.40t	0.999167	2.530E-08	294
h-h2o.41t	0.999167	2.444E-08	284
h-h2o.42t	0.999167	2.585E-08	300
h-h2o.43t	0.999167	2.789E-08	324
h-h2o.44t	0.999167	3.016E-08	350
h-h2o.45t	0.999167	3.220E-08	374

h-h2o.46t	0.999167	3.447E-08	400
h-h2o.47t	0.999167	3.650E-08	424
h-h2o.48t	0.999167	3.878E-08	450
h-h2o.49t	0.999167	4.081E-08	474
h-h2o.50t	0.999167	4.309E-08	500
h-h2o.51t	0.999167	4.512E-08	524
h-h2o.52t	0.999167	4.740E-08	550
h-h2o.53t	0.999167	4.943E-08	574
h-h2o.54t	0.999167	5.170E-08	600
h-h2o.55t	0.999167	5.374E-08	624
h-h2o.56t	0.999167	5.601E-08	650
h-h2o.57t	0.999167	6.894E-08	800
h-ice.40t	0.999167	9.910E-09	115
h-ice.41t	0.999167	1.621E-08	188
h-ice.42t	0.999167	1.794E-08	208
h-ice.43t	0.999167	1.966E-08	228
h-ice.44t	0.999167	2.009E-08	233
h-ice.45t	0.999167	2.138E-08	248
h-ice.46t	0.999167	2.182E-08	253
h-ice.47t	0.999167	2.311E-08	268
h-ice.48t	0.999167	2.354E-08	273
h-luci.40t	0.999167	2.585E-08	300
h-poly.40t	0.999167	2.530E-08	294
h-poly.41t	0.999167	6.635E-09	77
h-poly.42t	0.999167	1.689E-08	196
h-poly.43t	0.999167	2.008E-08	233
h-poly.44t	0.999167	2.585E-08	300
h-poly.45t	0.999167	2.611E-08	303
h-poly.46t	0.999167	2.697E-08	313
h-poly.47t	0.999167	2.783E-08	323
h-poly.48t	0.999167	2.870E-08	333
h-poly.49t	0.999167	2.783E-08	323
h-poly.50t	0.999167	2.870E-08	333
h-yh2.40t	0.999167	2.530E-08	294
h-yh2.41t	0.999167	3.447E-08	400
h-yh2.42t	0.999167	4.309E-08	500
h-yh2.43t	0.999167	5.170E-08	600
h-yh2.44t	0.999167	6.032E-08	700
h-yh2.45t	0.999167	6.894E-08	800
h-yh2.46t	0.999167	8.617E-08	1000
h-yh2.47t	0.999167	1.034E-07	1200
h-yh2.48t	0.999167	1.206E-07	1400
h-yh2.49t	0.999167	1.379E-07	1600
h-zrh.40t	0.999167	2.551E-08	296

h-zrh.41t	0.999167	3.447E-08	400
h-zrh.42t	0.999167	4.309E-08	500
h-zrh.43t	0.999167	5.170E-08	600
h-zrh.44t	0.999167	6.032E-08	700
h-zrh.45t	0.999167	6.894E-08	800
h-zrh.46t	0.999167	8.617E-08	1000
h-zrh.47t	0.999167	1.034E-07	1200
lmeth.40t	0.999167	8.617E-09	100
n-un.40t	13.88278	2.551E-08	296
n-un.41t	13.88278	3.447E-08	400
n-un.42t	13.88278	4.309E-08	500
n-un.43t	13.88278	5.170E-08	600
n-un.44t	13.88278	6.032E-08	700
n-un.45t	13.88278	6.894E-08	800
n-un.46t	13.88278	8.617E-08	1000
n-un.47t	13.88278	1.034E-07	1200
o-beo.40t	15.85751	2.530E-08	294
o-beo.41t	15.85751	3.447E-08	400
o-beo.42t	15.85751	4.309E-08	500
o-beo.43t	15.85751	5.170E-08	600
o-beo.44t	15.85751	6.032E-08	700
o-beo.45t	15.85751	6.894E-08	800
o-beo.46t	15.85751	8.617E-08	1000
o-beo.47t	15.85751	1.034E-07	1200
o-d2o.40t	15.85751	2.530E-08	294
o-d2o.41t	15.85751	2.444E-08	284
o-d2o.42t	15.85751	2.585E-08	300
o-d2o.43t	15.85751	2.789E-08	324
o-d2o.44t	15.85751	3.016E-08	350
o-d2o.45t	15.85751	3.220E-08	374
o-d2o.46t	15.85751	3.447E-08	400
o-d2o.47t	15.85751	3.650E-08	424
o-d2o.48t	15.85751	3.878E-08	450
o-d2o.49t	15.85751	4.081E-08	474
o-d2o.50t	15.85751	4.309E-08	500
o-d2o.51t	15.85751	4.512E-08	524
o-d2o.52t	15.85751	4.740E-08	550
o-d2o.53t	15.85751	4.943E-08	574
o-d2o.54t	15.85751	5.170E-08	600
o-d2o.55t	15.85751	5.374E-08	624
o-d2o.56t	15.85751	5.601E-08	650
o-ice.40t	15.85751	9.910E-09	115
o-ice.41t	15.85751	1.621E-08	188
o-ice.42t	15.85751	1.794E-08	208

o-ice.43t	15.85751	1.966E-08	228
o-ice.44t	15.85751	2.009E-08	233
o-ice.45t	15.85751	2.138E-08	248
o-ice.46t	15.85751	2.182E-08	253
o-ice.47t	15.85751	2.311E-08	268
o-ice.48t	15.85751	2.354E-08	273
o-uo2.40t	15.85751	2.551E-08	296
o-uo2.41t	15.85751	3.447E-08	400
o-uo2.42t	15.85751	4.309E-08	500
o-uo2.43t	15.85751	5.170E-08	600
o-uo2.44t	15.85751	6.032E-08	700
o-uo2.45t	15.85751	6.894E-08	800
o-uo2.46t	15.85751	8.617E-08	1000
o-uo2.47t	15.85751	1.034E-07	1200
orthod.40t	1.9968	1.637E-09	19
orthoh.40t	0.999167	1.724E-09	20
parad.40t	1.9968	1.637E-09	19
parah.40t	0.999167	1.724E-09	20
si-sic.40t	27.737	2.585E-08	300
si-sic.41t	27.737	3.447E-08	400
si-sic.42t	27.737	4.309E-08	500
si-sic.43t	27.737	5.170E-08	600
si-sic.44t	27.737	6.032E-08	700
si-sic.45t	27.737	6.894E-08	800
si-sic.46t	27.737	8.617E-08	1000
si-sic.47t	27.737	1.034E-07	1200
sio2.40t	15.85751	2.530E-08	294
sio2.41t	15.85751	3.016E-08	350
sio2.42t	15.85751	3.447E-08	400
sio2.43t	15.85751	4.309E-08	500
sio2.44t	15.85751	6.894E-08	800
sio2.45t	15.85751	8.617E-08	1000
sio2.46t	15.85751	9.479E-08	1100
smeth.40t	0.999167	1.896E-09	22
u-un.40t	236.0058	2.551E-08	296
u-un.41t	236.0058	3.447E-08	400
u-un.42t	236.0058	4.309E-08	500
u-un.43t	236.0058	5.170E-08	600
u-un.44t	236.0058	6.032E-08	700
u-un.45t	236.0058	6.894E-08	800
u-un.46t	236.0058	8.617E-08	1000
u-un.47t	236.0058	1.034E-07	1200
u-uo2.40t	236.0058	2.551E-08	296
u-uo2.41t	236.0058	3.447E-08	400

u-uo2.42t	236.0058	4.309E-08	500
u-uo2.43t	236.0058	5.170E-08	600
u-uo2.44t	236.0058	6.032E-08	700
u-uo2.45t	236.0058	6.894E-08	800
u-uo2.46t	236.0058	8.617E-08	1000
u-uo2.47t	236.0058	1.034E-07	1200
y-yh2.40t	88.1421	2.530E-08	294
y-yh2.41t	88.1421	3.447E-08	400
y-yh2.42t	88.1421	4.309E-08	500
y-yh2.43t	88.1421	5.170E-08	600
y-yh2.44t	88.1421	6.032E-08	700
y-yh2.45t	88.1421	6.894E-08	800
y-yh2.46t	88.1421	8.617E-08	1000
y-yh2.47t	88.1421	1.034E-07	1200
y-yh2.48t	88.1421	1.206E-07	1400
y-yh2.49t	88.1421	1.379E-07	1600
zr-zrh.40t	89.1324	2.551E-08	296
zr-zrh.41t	89.1324	3.447E-08	400
zr-zrh.42t	89.1324	4.309E-08	500
zr-zrh.43t	89.1324	5.170E-08	600
zr-zrh.44t	89.1324	6.032E-08	700
zr-zrh.45t	89.1324	6.894E-08	800
zr-zrh.46t	89.1324	8.617E-08	1000
zr-zrh.47t	89.1324	1.034E-07	1200

A typical input file used for processing in NJOY is given below. This file calculates the ACE files for MCNP and produces the xsdir input lines for the first 2 temperature of H in H_2O. Also note that all of the temperatures can be processed at the same time by thermr, while acer can only process 1 temperature at a time. The second acer run is for data checking and printing of detailed results.

Also note that the regular neutron cross section evaluation file is input via “tape20” and the tsl evaluation file is input via “tape30” into thermr.

```
moder
    20 -21
reconr
    -21 -22
    'pendf tape for ENDF/B-VIII 1-H-1'/
    125 7 0/
    .001/
    '1-H-1 from ENDF/B-VIII'/
    'the following reaction types are added'/
    '     mt20x   gas production'/
    '     mt221   free thermal scattering'/
```

```
    '     mt301   total heating kerma factor'/
    '     mt443   kinematic kerma'/
    '     mt444   total damage energy production'/
    0/
broadr
    -21 -22 -23
    125 9/
    .001/
    283.6 293.6 300 323.6 350 373.6 400 423.6 450 /
    0/
heatr
    -21 -23 -24/
    125 4/
    302 402 443 444 /
thermr
    30 -24 -25
    1 125 20 9 2 0 0 2 227 1 /
    283.6 293.6 300 323.6 350 373.6 400 423.6 450 /
    .001 10.00008/
gaspr
    -21 -25 -27
moder
    -27 28
    -- Tape 5x is the actual ACE file
    -- Tape 6x is the XSDIR entry
acer
    30 28 0 52 62
    2 0 1 .81/
    'H in H2O at 283.6k ' /
    125 283.6 'h-h2o' 1
    1001/
    227 80 0 0 1 10.00008 2/
    -- Tape 7x is the "tested" ACE file
    -- Tape 8x is the "tested" XSDIR entry
acer
    0 52 92 72 82/
    7 1/
    'H in H2O at 283.6k ' /
    --
    -- Tape 5x is the actual ACE file
    -- Tape 6x is the XSDIR entry
viewr
    92 42
acer
    30 28 0 51 61
    2 0 1 .80/
    'H in H2O at 293.6k ' /
    125 293.6 'h-h2o' 1
    1001/
    227 80 0 0 1 10.00008 2/
    -- Tape 7x is the "tested" ACE file
    -- Tape 8x is the "tested" XSDIR entry
acer
    0 51 91 71 81/
```

```
    7 1/
    'H in H2O at 293.6k ' /
    --
    -- Tape 5x is the actual ACE file
    -- Tape 6x is the XSDIR entry
viewr
    91 41
```

Inputs for a MCNP xsdir directory file were also generated for each of the 253 ACE files. In the installation of these tables, some of the relative file addresses may need to be modified to match the local computer file system.

III. Initial Verification of the Re-Released S(α,β) Library

The initial verification of the re-processed S(α,β) files was to plot the cross sections below and at Emax to verify the (relatively) smooth transition from higher incident neutron energy free gas modelling to the lower incident neutron energy thermal scattering law. Some sample plots are given below.

If the interactive plotter of MCNP is not available, the data points may be found in the ACER printed outputs (with the default iprint=1 flag in position 2 of card 2). In the sample deck shown above, this print edit is produced by the second acer run. In the print edit, incoherent inelastic reaction cross sections as a function of incident neutron energy can be extracted by searching for the string, "incident energy". Coherent elastic reaction cross sections can be located by searching for the string "bragg". Incoherent elastic reaction cross sections can be located by searching for the string "incoherent". The "total" S(α,β) cross sections are not edited per se because the energy grids of the component pieces are not defined on the same energy grid.

Curiously, the cross section multipliers for tallies in MCNP can only access the "total" S(α,β) scattering (using mt 2) and are unable to access the individual elastic or inelastic components.

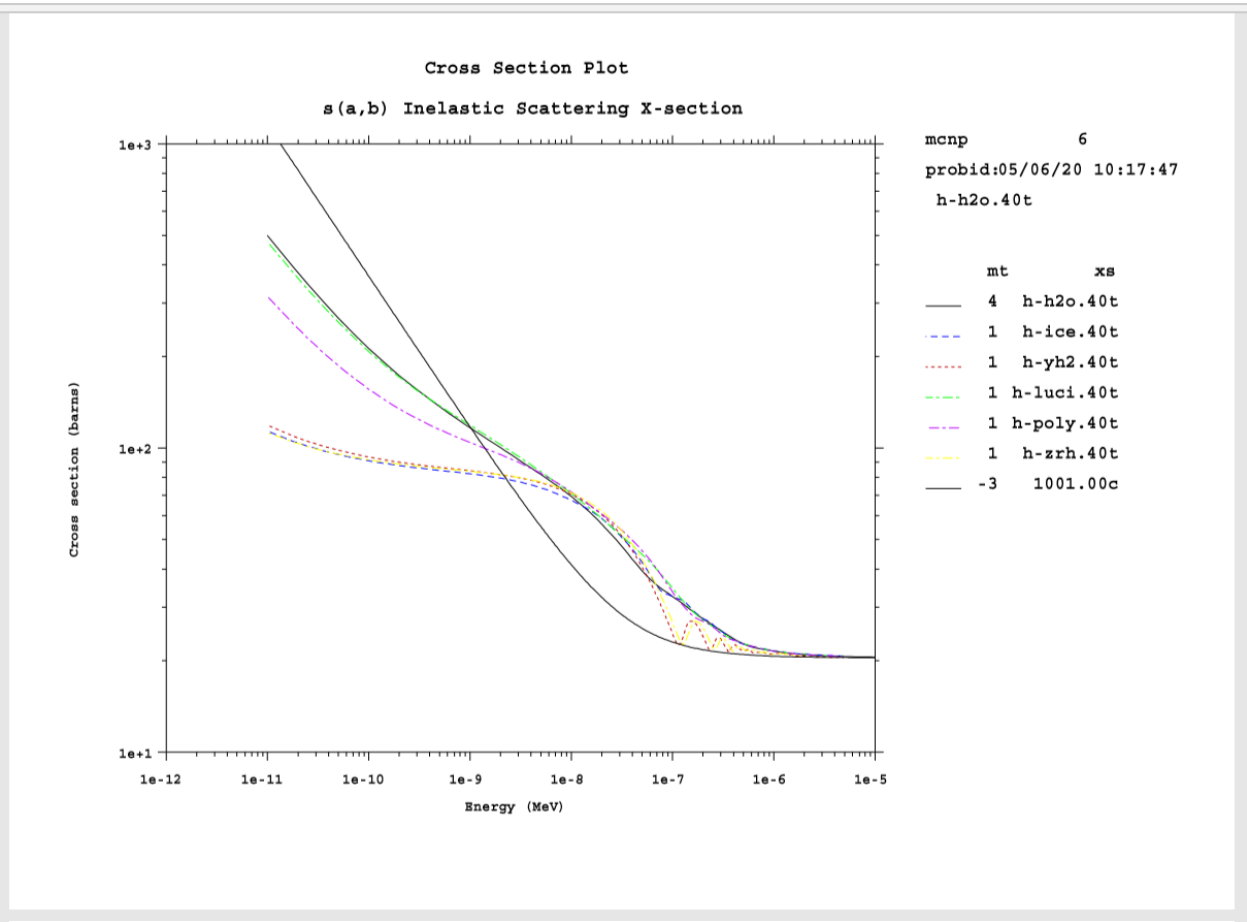

Figure 1: Consistency between S(α,β) data and free gas data for H in Various Compounds

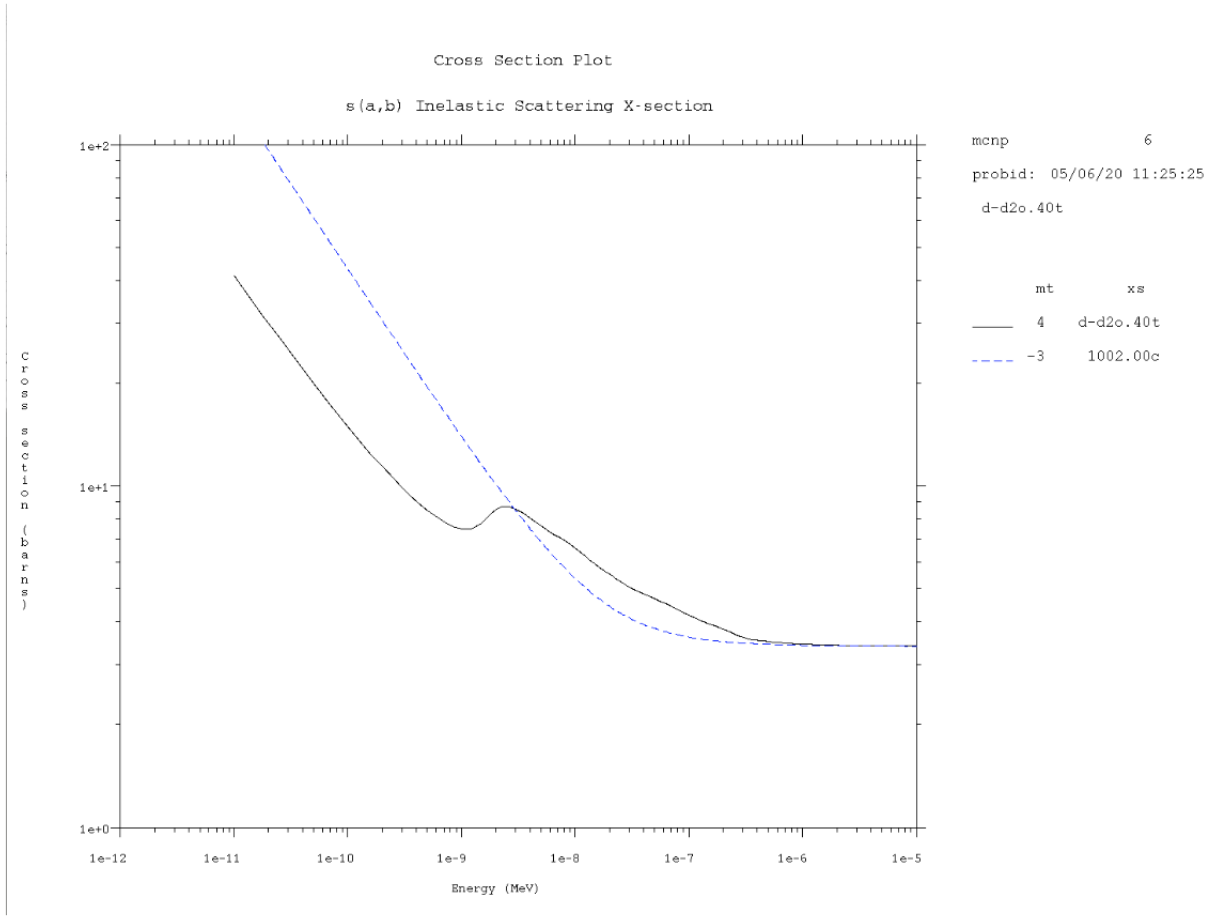

Figure 2: Consistency of D S(α,B) data with free gas data in D_2O

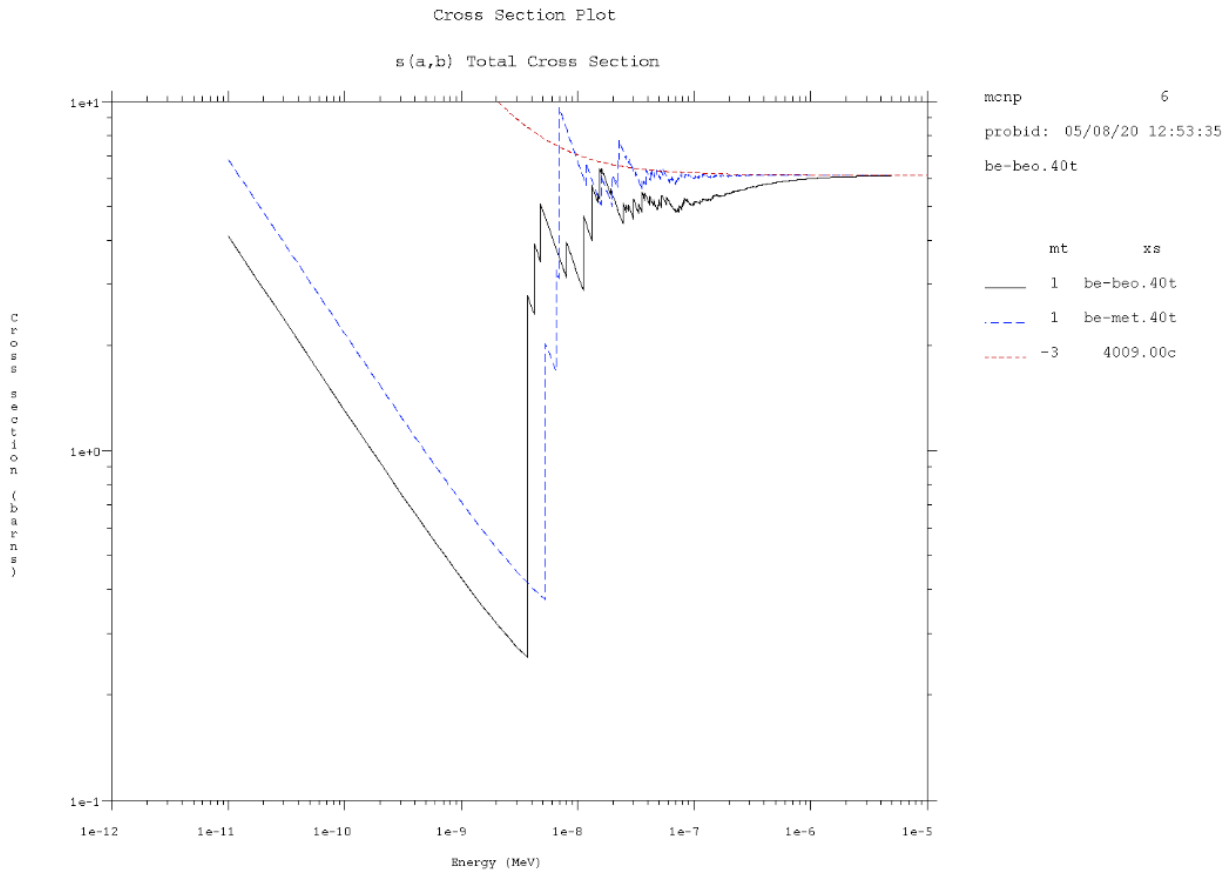

Figure 3: Consistency of Be S(α,β) data with free gas data in Various Compounds

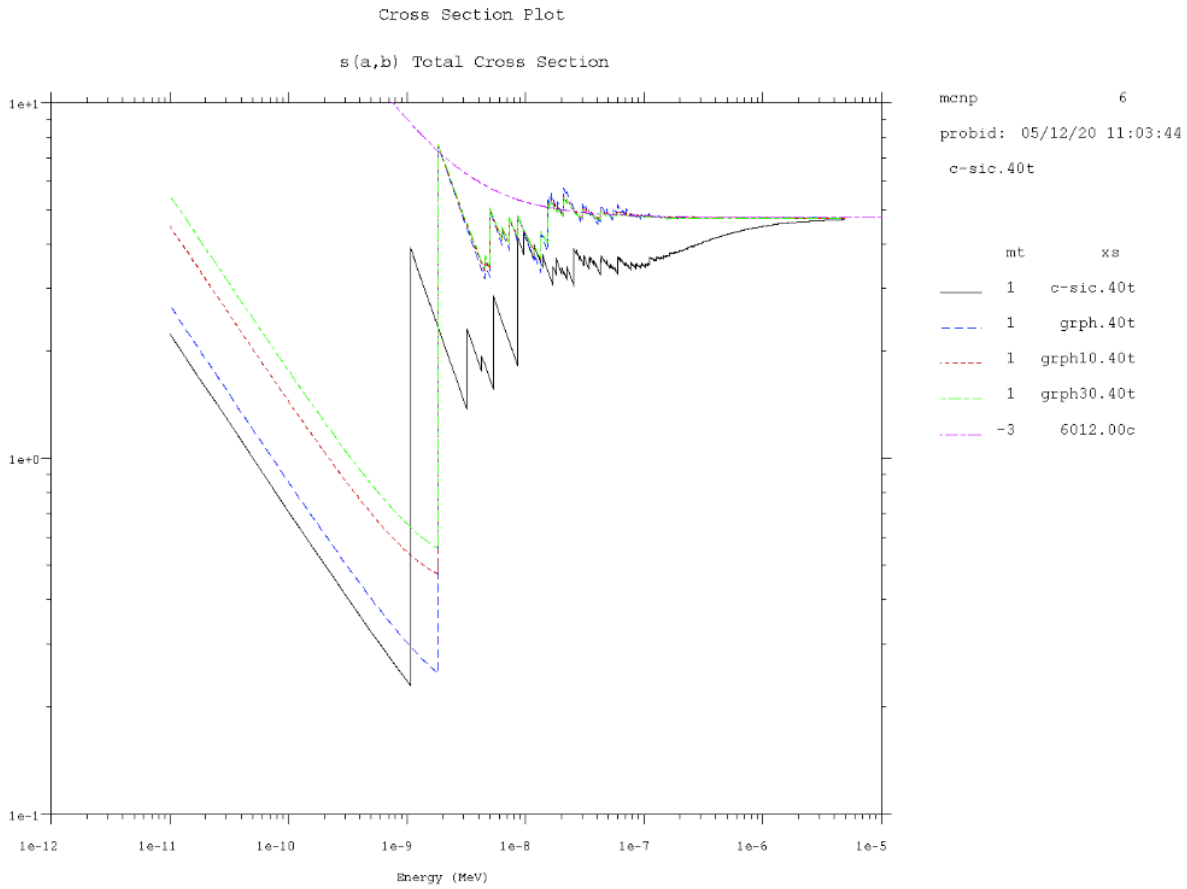

Figure 4: Consistency of C S(α,β) data with free gas data in Various Compounds

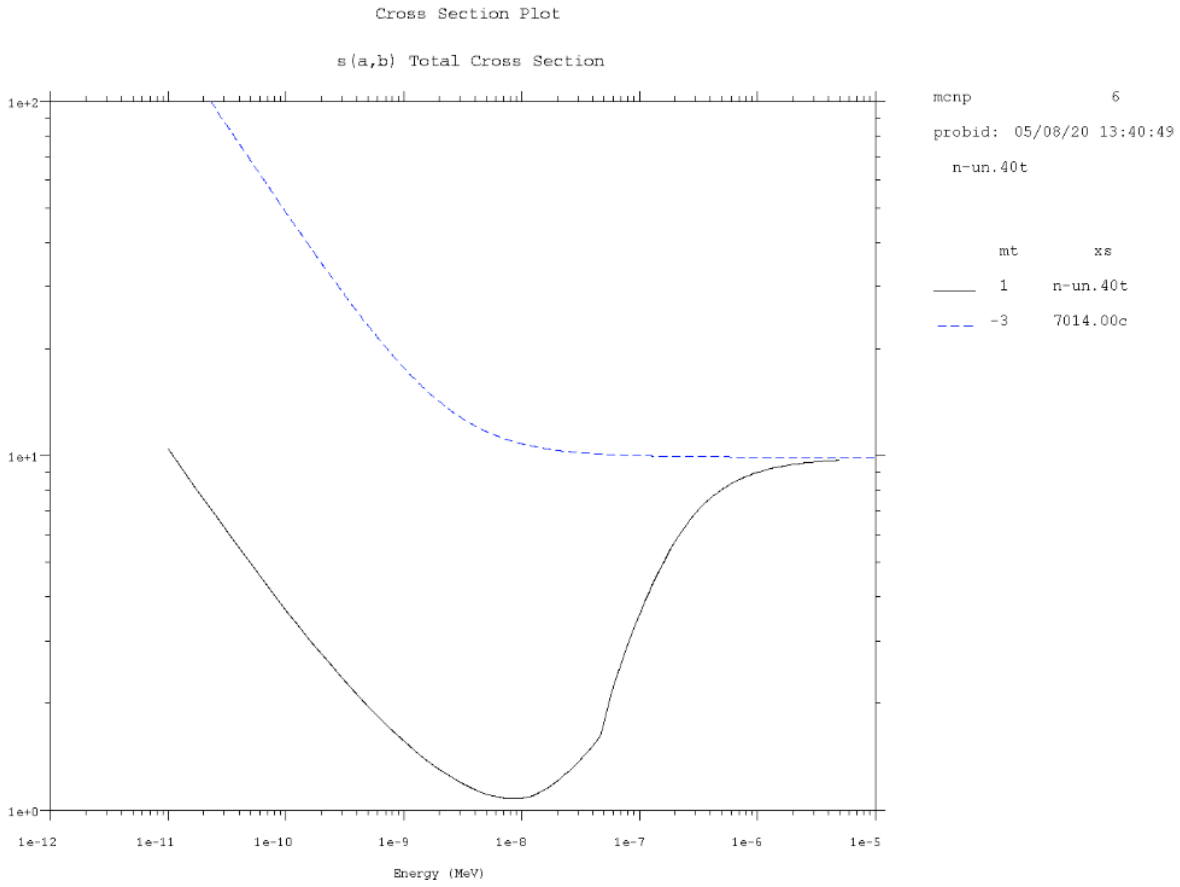

Figure 5: Consistency of N S(α,β) data with free gas data in N-UN

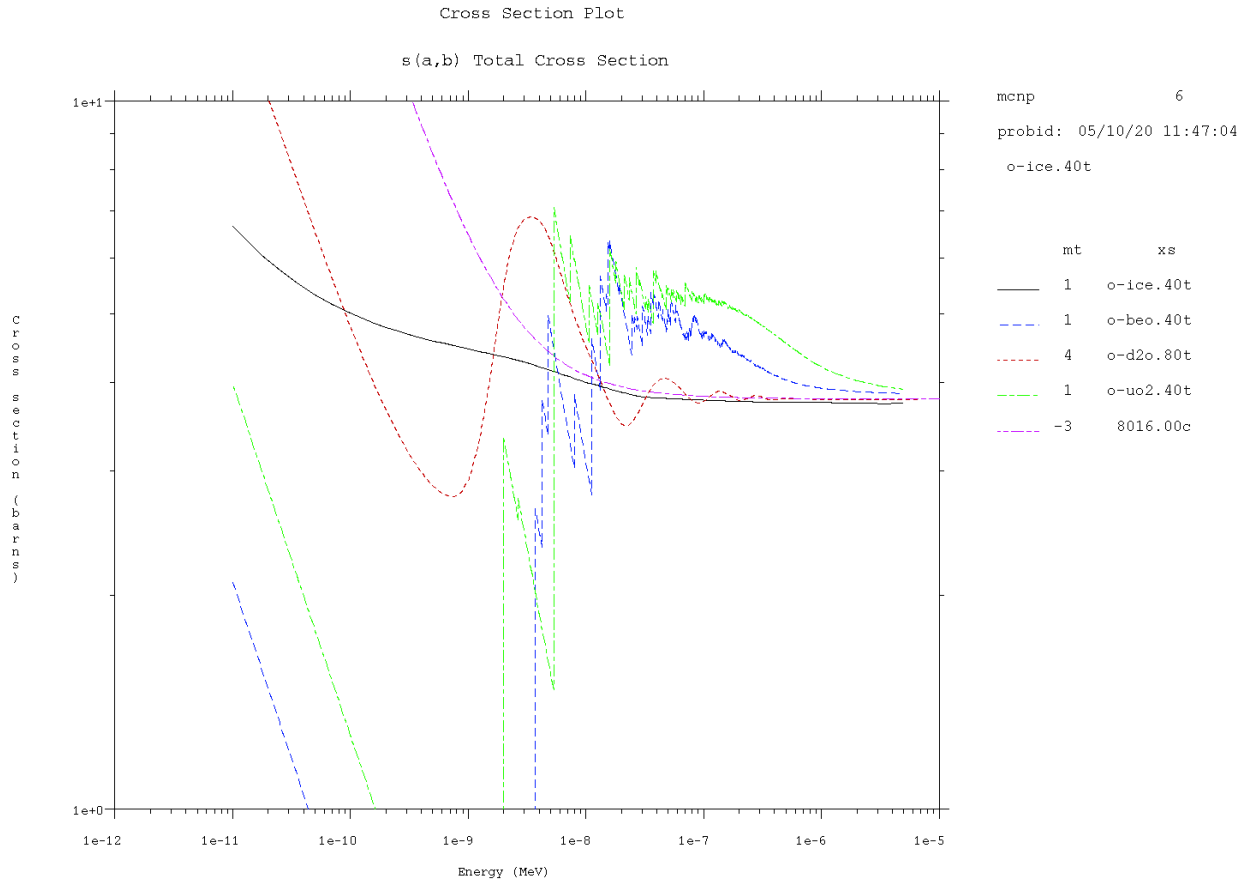

Figure 6: Consistency of O S(α,β) data with free gas data in Various Compounds

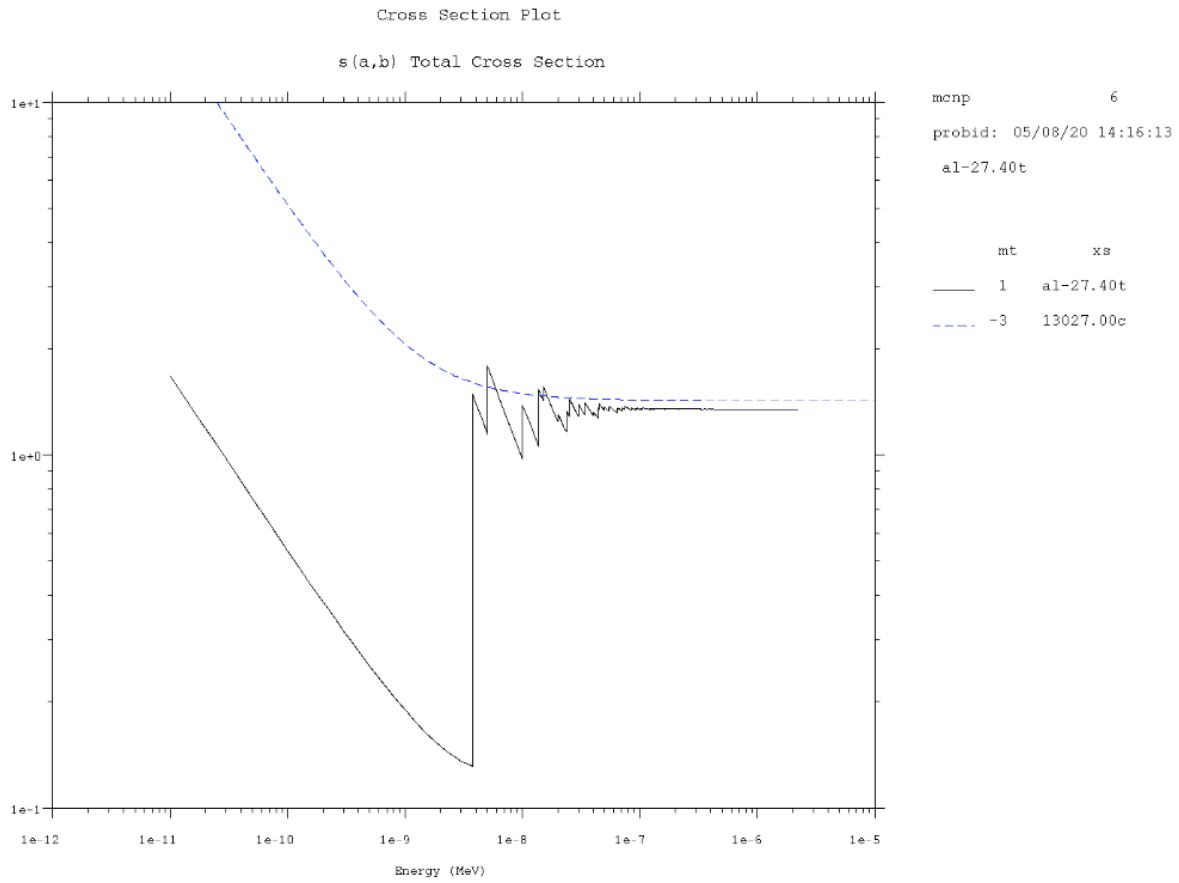

Figure 7: Consistency of Al S(α,β) data with free gas data

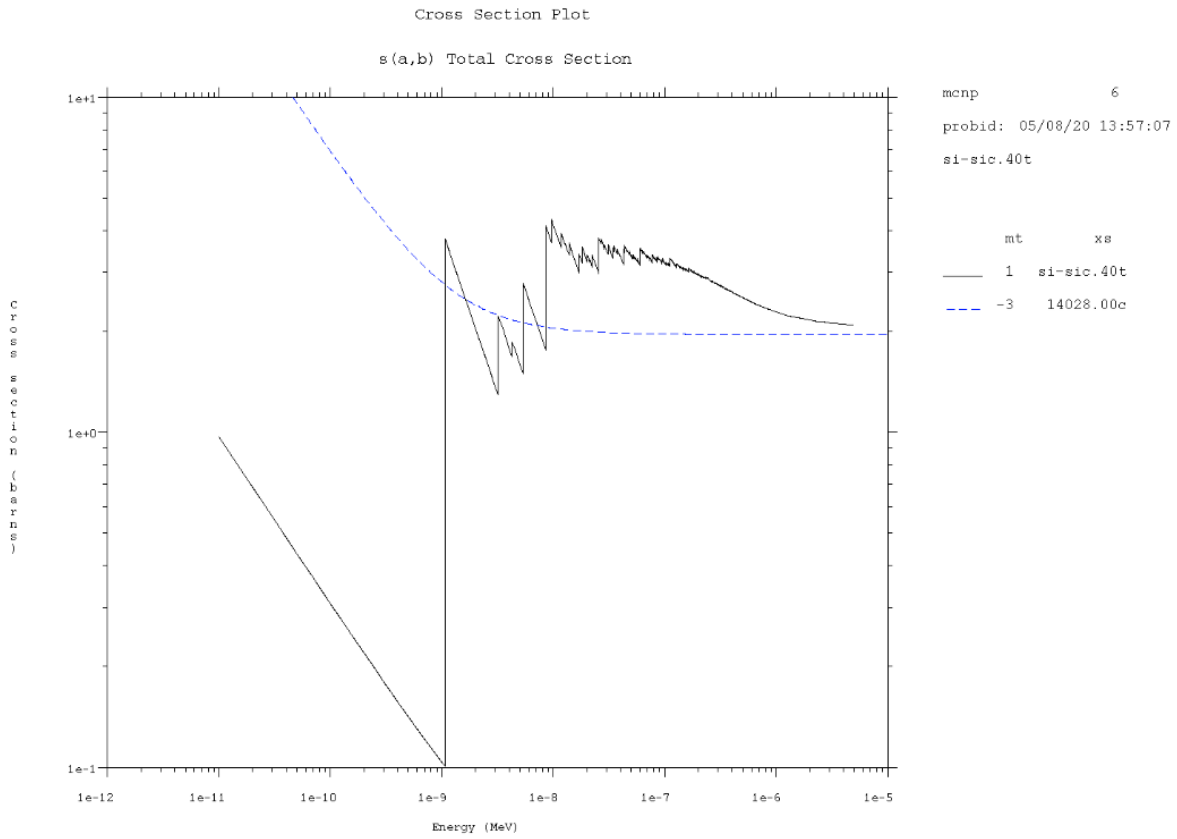

Figure 8: Consistency of Si S(α,β) data with free gas data

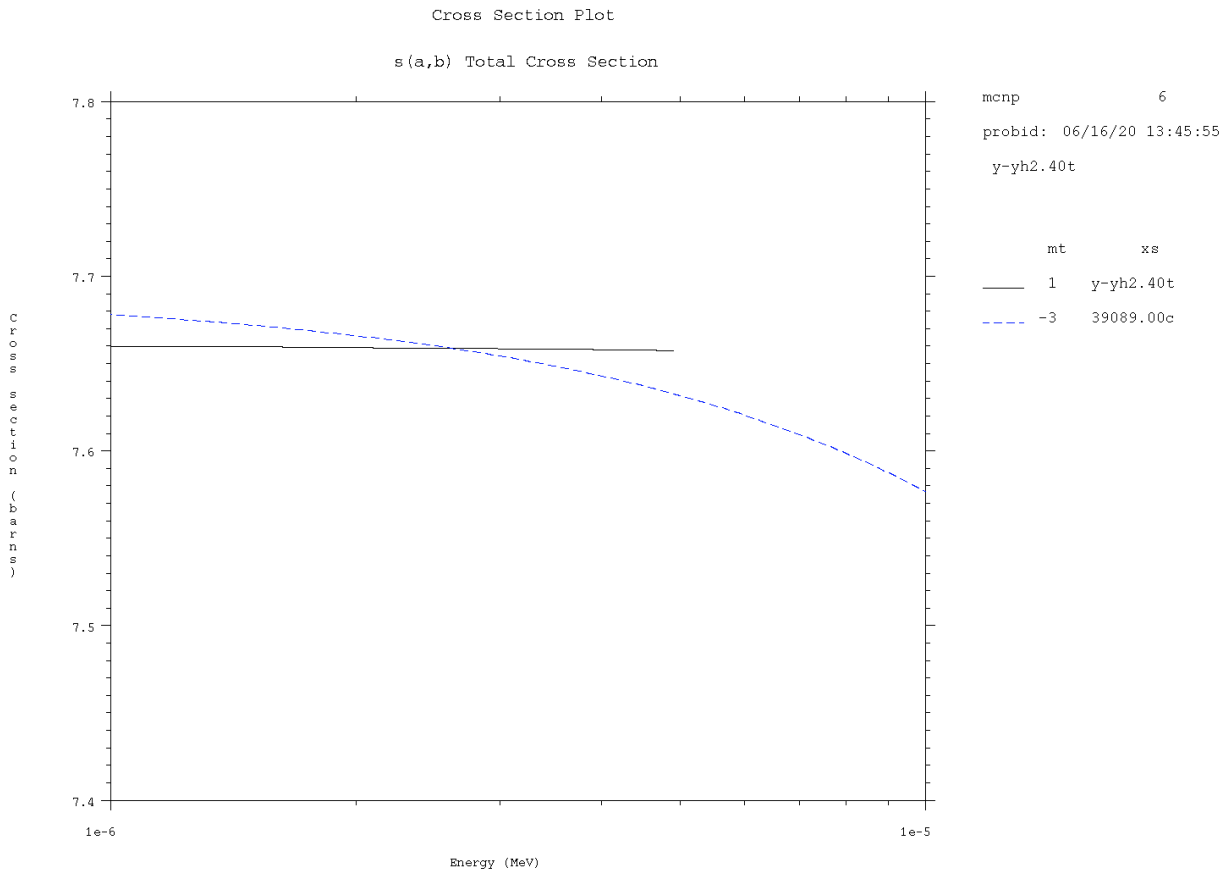

Figure 9: Consistency of Y S(α,β) data with free gas data

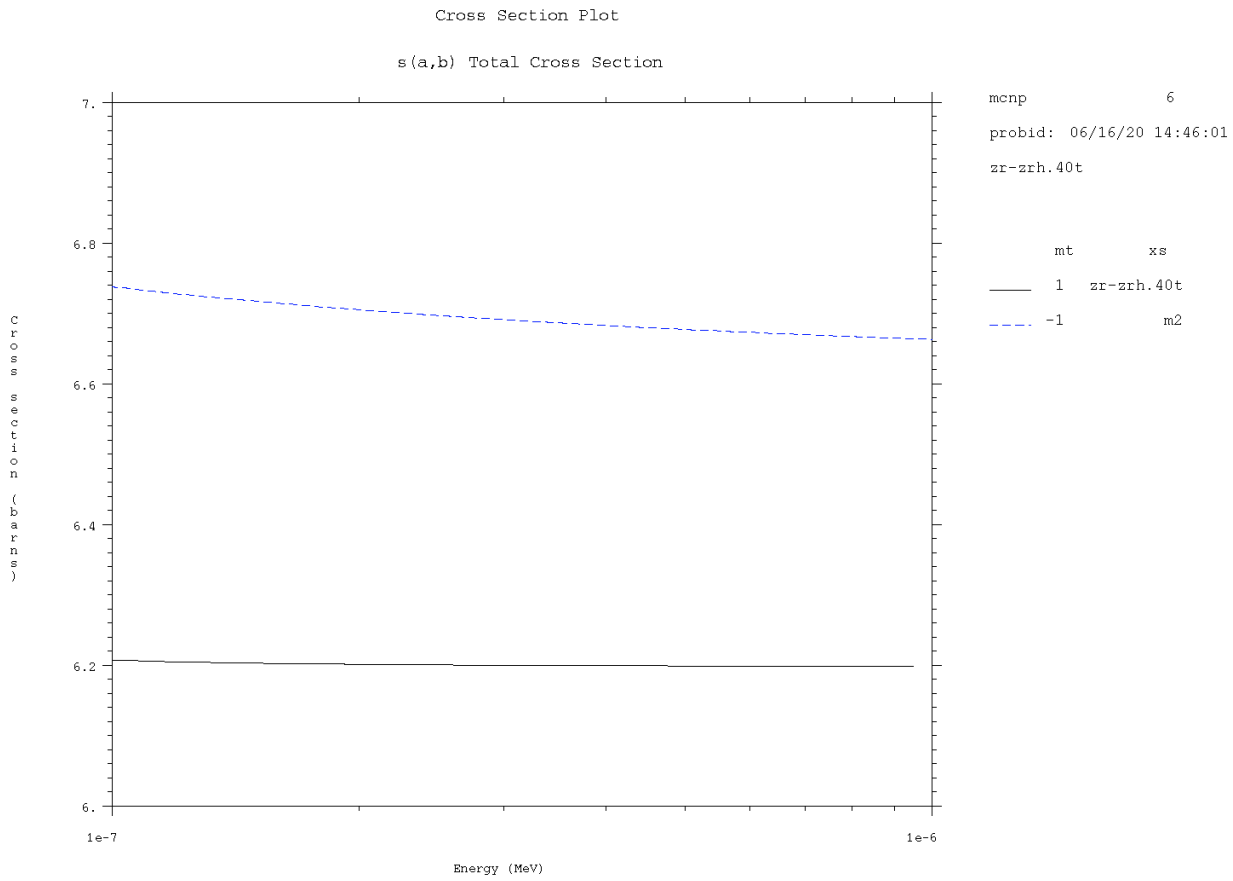

Figure 10: Reasonable Consistency of Zr S(α,β) data with elemental Zr free gas data

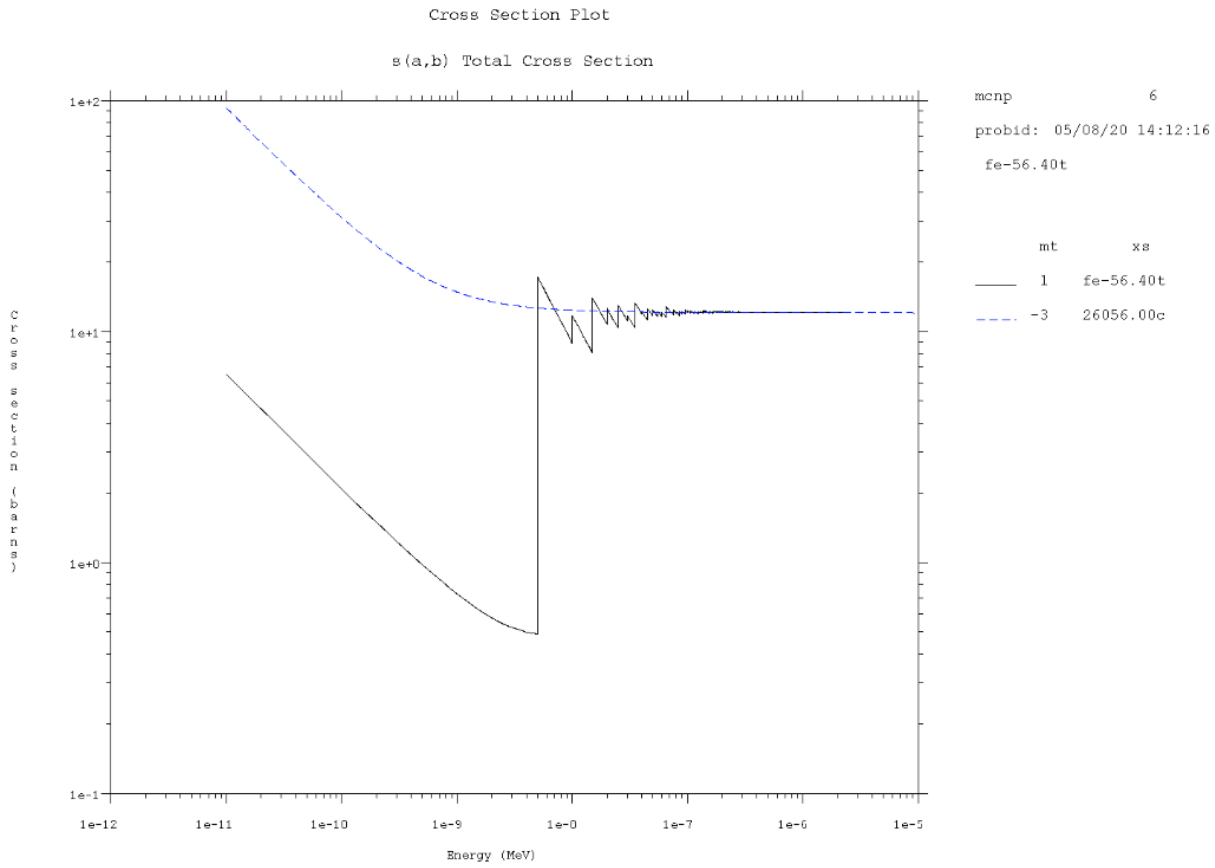

Figure 11: Consistency of Fe S(α,β) data with free gas data

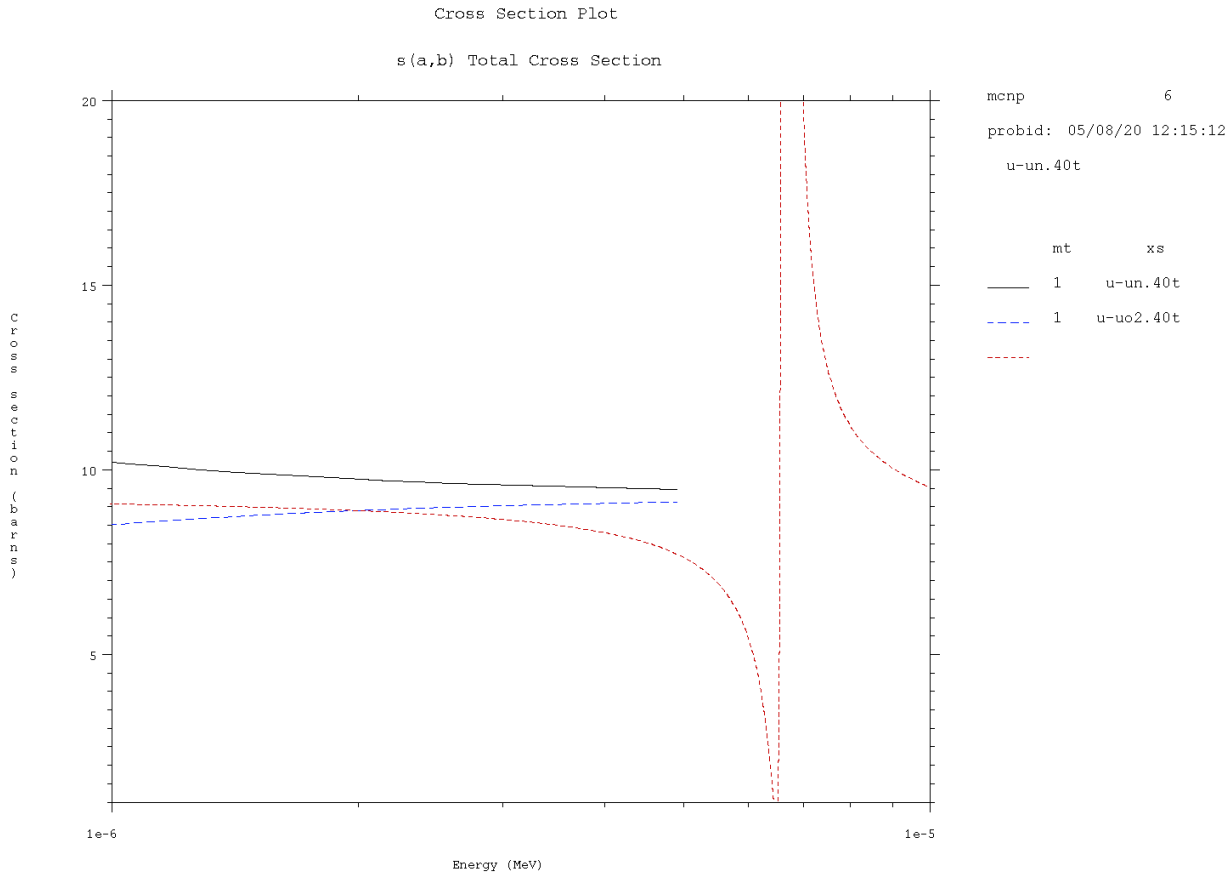

Figure 12: Partial Consistency of U S(α,β) data with free gas data

IV. Major Problems with the Original Release

When the ENDF/B VIII.0 thermal scattering files were originally processed[5] with NJOY, there were quite a few inadvertent bugs in the data files. A considerable amount of helpful feedback was received and corrections were eventually made. What follows is a description of the major problems discovered and the corrections which were made.

(1) Reversal of grph10 and grph30

In the original release, the ACE files for grph10 and grph30 were reversed. This was first pointed out by Kontogeorgakos Dimitris in June 2018 and has since been corrected.

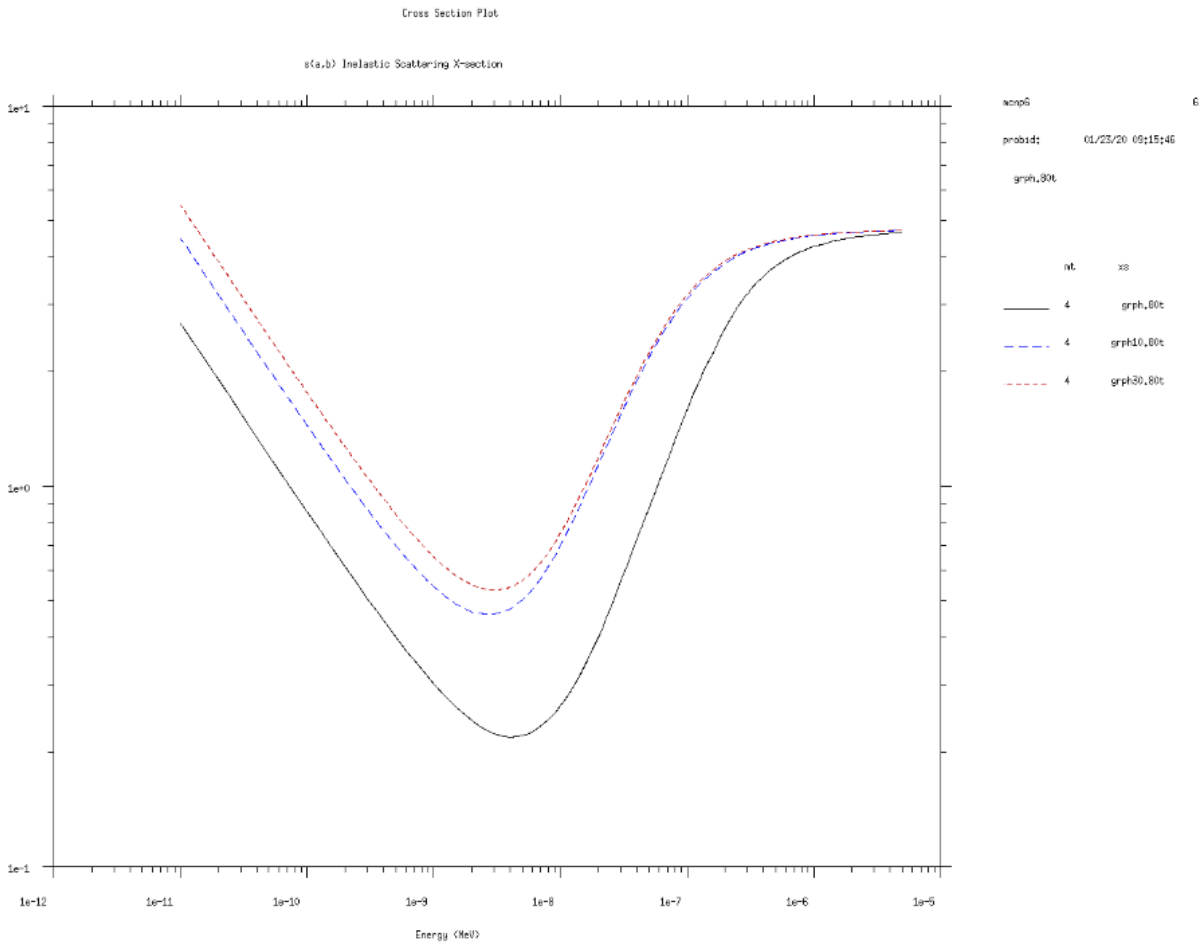

Figure 13: Verification of the Graphite Identifications by Inelastic Scattering

(2) Problems with incoherent thermal elastic scattering

Paul Romano (November 2019) and Lei Zheng (April 2019) pointed this problem out in h-zrh. The problem was an incorrect ACER input for all materials with incoherent thermal elastic scattering. The explanation and list of affected materials follows below.

In the thermal scattering law (tsl) file from National Nuclear Data Center (nndc.bnl.gov), there will be a MF 7 MT 4 section – which is inelastic incoherent scattering. All tsl files have this. There may or may not be a MF 7 MT 2 section – which is either coherent or incoherent elastic scattering, or no elastic scattering at all. Coherent elastic scatterers will typically have a much larger MF 7 MT 2 section than the incoherent elastic scatterers, due to the details of the Bragg edges. The actual flag on the tsl file is LTHR = 1 or 2 = coherent or incoherent elastic scattering on card 1 of the MF 7 MT 2 section – third position.

Using an arbitrary MT of 227 (and 228) from the range of S(α,β) values in NJOY, the MF 7 MT 4 section corresponds with 227. If present, the elastic scattering in MF 7 and MT 2 will correspond to 228.

NJOY ACER card 9 has the following inputs:

MTI for thermal inelastic incoherent scattering

NBINT number of bins for incoherent scattering

MTE for thermal elastic scattering

IELAS 0/1 = coherent / incoherent thermal elastic scattering

…

Examples of NJOY ACER Card 9:

227 80 228 0 …. Coherent elastic scattering (should see Bragg edges)

227 80 228 1 … Incoherent elastic scattering

227 80 0 0 … No elastic scattering

…

ENDF/B VIII.0 thermal scattering law (tsl) materials:

Coherent elastic scattering is found in Al, Fe, Be, BeO, Graphite, UO_2, SiC, and SiO_2.

Incoherent elastic scattering is found in ZrH, poly (CH_2), lucite ($C_5O_2H_8$), YH_2, Ice, solid methane (sCH_4), and N in UN,

No thermal elastic scattering is found in H_2O, D_2O, liquid methane (lCH_4), benzene (C_6H_6), ortho and para H and D,

UN has incoherent elastic scattering for N in UN, but coherent elastic scattering for U in UN.

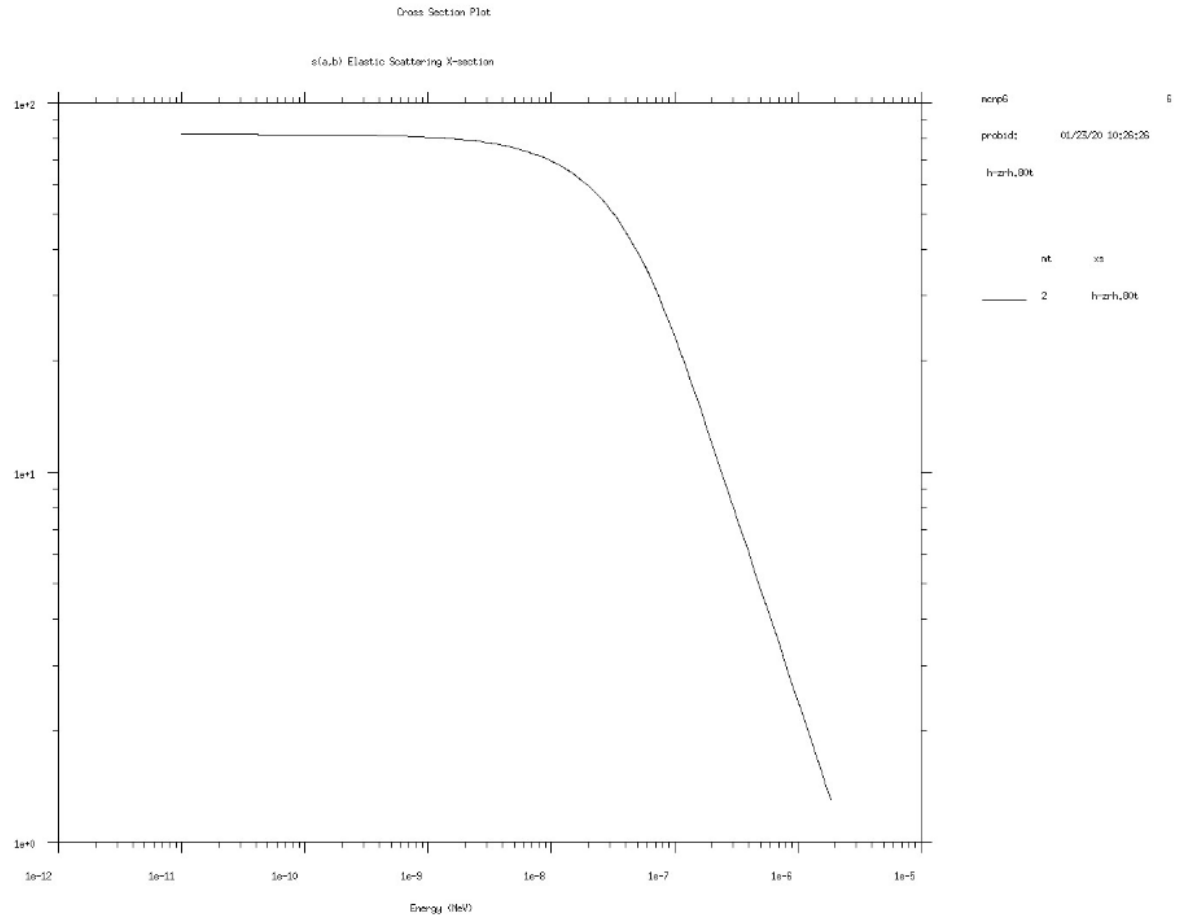

Figure 14: Verification of the Incoherent Elastic Scattering of H in Zirc-Hydride

(3) SiO_2 problems in processing

Alyssa Kersting (Nov 2018) pointed out this problem early on and Jesse Holmes helped with its resolution. For ENDF/B VIII.0, there are 2 compounds in the S(α,β) list – SiO_2 and benzene. Furthermore, the tsl file for SiO_2 assumes that the tape20 file used in NJOY processing will be Si, not O.

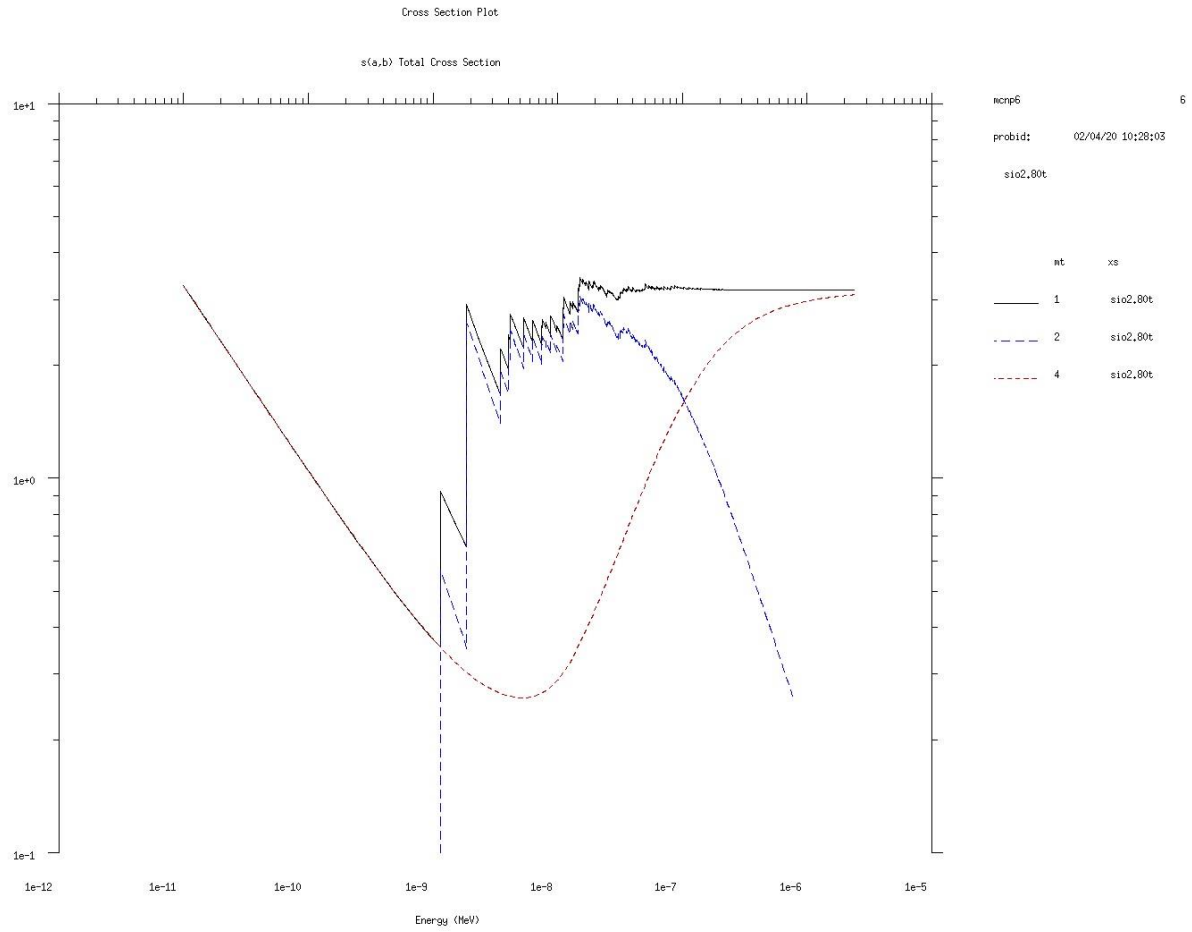

Figure 15: Decomposition of the SiO_2 S(α,β) Data

(4) H-Poly at the 2 highest temperatures

In the original release, the highest 2 temperatures for h-poly were duplicates of the next 2 lower temperatures. This problem was brought to our attention by Paul Romano in July 2019. It has been fixed.

(5) Inadvertent Omission of 5 higher temperature data files

In the original release; the highest temperature data for the 3 graphite's and the 2 yttrium hydrides (thus, grph.89t, grph10.89t, grph30.89t, h-yh2.89t, and y-yh2.89t) were not processed. They have since been included – changing the total number of files from 248 to 253.

V. New Feature in NJOY

With the most recent versions on NJOY2016 (beyond about version 27), card 8 of the NJOY ACER input has an additional value in the 4th position – NZA. It is the number of ZA's coming on card(s) 8a. Values for NZA between 1 and 16 are acceptable. This eliminates the long-standing limitation of NJOY to allow only three ZAID substitutions for thermal scattering data and makes the ACE files more consistent with MCNP's ability to handle up to 16 substitutions.

VI. Further Verification of the Re-Released S(α,β) Data with MCNP Test Problems

In order to further verify the thermal scattering data and its use in MCNP, test problems with all of the tsl materials were run and analyzed. The basic test problem setup in MCNP is a fixed source problem in an effectively infinite homogeneous media of the tsl material of interest. A fixed neutron source is set as a Maxwellian distribution at the material temperature and analog capture is set in the PHYS:n card. Thus, the neutron population is initially set to thermal energies; there is no slowing down from fission energies.

Tallies are set up for the F4 flux, the inverse velocity weighted flux (F14), and flux-weighted cross sections using the multipliers on a flux tally (F24). A sample deck for light water at 600K follows. MCNP version 6.2.1 has been used in these calculations.

```
test deck for ENDF/B VIII S(α,β) in MCNP
1     1       -1.00           -1    imp:n=1
2     0                  1          imp:n=0

1     so    10000.0

sdef  pos=0 0 0 erg=d1 nrm=1.0
sp1   -2   5.17e-8
nps   1000000
print
tmp     5.17e-8  5.17e-8
m1      1001.01    2.0     8016.01   1.0
mt1     h-h2o.54t
f4:n      1
e4   1.0e-10 2298i 2.3e-7  100   T
f14:n  1
fm14   1 -2
phys:n  20 20
f24:n  1
fm24   (1.0 1 1) (1.0 1 2)
```

The neutron lifetime from MCNP on this sample problem will correspond to the thermal diffusion time for the moderator. Values were measured many years ago[6] for the thermal diffusion time in common moderators. While these old data (based on theory and some measurements) are not very precise, and the presence of impurities in the moderators (e.g., H in D2O, and B in Graphite) can also affect the results, it is still the case that the thermal diffusion

times should be approximately consistent between the MCNP6 calculation and the published data. Furthermore, the theory predicts that the diffusion time will be independent of the scattering cross section. It is only dependent on the inverse macroscopic capture cross section and the average neutron velocity. It can also be thought of as the ratio of the average distance travelled by the neutron (i.e., the capture mean free path (mfp)) divided by the average neutron velocity.

Therefore, the S(α,β) results should be the same as the free gas results for the thermal diffusion time. The results below in Table 3 are consistent with these expectations.

Tables 3: S(α,β) and free gas calculations of the thermal diffusion time ("t_d")

moderator	density (g/cc)	published t_d (sec)	S(α,β)	average lifetime (sec)	average no. of collisions	mfp (cm)
H_2O	1.00	2.10E-04	h	2.04E-04	163	0.333
D_2O	1.10	1.40E-01	d, o	1.16E-01	11428	2.573
D_2O	1.10	1.40E-01	d	1.16E-01	13280	2.204
D_2O	1.10	1.40E-01	o	1.16E-01	11711	2.510
Be	1.85	3.00E-03	be	3.67E-03	682	1.641
BeO	2.96	6.70E-03	be, o	6.25E-03	1079	1.704
BeO	2.96	6.70E-03	be	6.25E-03	984	1.586
BeO	2.96	6.70E-03	o	6.25E-03	1281	1.251
Graphite	1.60	1.70E-02	gr30	1.47E-02	1400	2.656
Graphite	2.00		gr10	1.17E-02	1412	2.115
Graphite	2.20		cgr	1.07E-02	1415	1.954

moderator	density (g/cc)	published t_d (sec)	neutron file	average lifetime (sec)	average no. of collisions	mfp (cm)
H_2O	1.00	2.10E-04	free gas	2.04E-04	106	0.502
D_2O	1.10	1.40E-01	free gas	1.16E-01	11673	2.511
Be	1.85	3.00E-03	free gas	3.67E-03	734	1.250
BeO	2.96	6.70E-03	free gas	6.25E-03	1152	1.352
Graphite	1.60	1.70E-02	free gas	1.47E-02	1450	2.525
Graphite	2.00		free gas	1.17E-02	1450	2.020
Graphite	2.20		free gas	1.07E-02	1450	1.836

VII. A Neutron Moderator in which all Cross Sections are Independent of Energy

In a simplified moderator where all neutron cross sections are constant, i.e., independent of energy, exact relationships between the various MCNP output results can be written. (With the assumption of "flat" cross sections, all neutrons will also have the same velocity.) The only cross sections present in this simplified moderator are total, scattering, and capture:

$$\Sigma_t = \Sigma_s + \Sigma_c \quad (1)$$

where the cross sections are macroscopic (inverse cm).

The neutron lifetime (or thermal diffusion time) is defined as

$$t_d = 1/v * 1/\Sigma_c = \lambda_c / v \quad (2)$$

where v = velocity (usually cm/sh),

- Σ_c = the macroscopic cross section (usually inverse cm),
- λ_c = the capture mfp (usually cm).

The average number of collisions (NC) for a neutron in this moderating material is

$$NC = 1 / (1 - SR) \quad (3)$$

where SR = scattering ratio = Σ_s / Σ_t .

This result can be deduced from the infinite series representation of $1 + x + x^2 + \ldots$ where the absolute value of x is < 1.0. The sum represents a starting collision plus the next collision for SR neutrons plus the next collision for SR^2 neutrons plus the next collision for SR^3 neutrons …

From these results the total, scattering, and capture cross sections can all be defined (after some algebra) in terms of MCNP-like quantities – the number of collisions (NC), the neutron lifetime (t_d), and the neutron velocity (v).

$$\Sigma_t = NC / v / t_d \quad (4)$$

$$\Sigma_s = (NC - 1) / v / t_d \quad (5)$$

$$\Sigma_c = 1 / v / t_d \quad (6)$$

To convert these macro cross sections (inverse cm) into micro cross sections (barns per atom), simply divide by the number density of atoms (atoms/barn/cm). Equation 6 is just the definition of the thermal diffusion time. By analogy, then, Equations 4 and 5 are logical extensions of that definition for the total and scattering cross sections. If Equations 4 and 5 are rewritten in terms of neutron lifetime:

$$t_d = NC * \lambda_t / v \quad (7)$$

$$t_d = (NC - 1) * \lambda_s / v \quad (8)$$

where λ_t = the total mean free path,

and λ_s = the scattering mean free path.

The scattering ratio can also be defined in terms of the number of collisions as follows:

$$SR = (NC - 1) / NC \quad (9)$$

VIII. Back to the Real World of Neutron Moderators

Of course, neutron cross sections are not independent of energy. Not all neutrons travel at the same velocity. However, if the constant cross sections and velocity are replaced by averaged cross sections and velocities, the relationships derived above are still pretty good approximations to the behavior of neutrons in real moderators.

It is a very good approximation because two the three foundational equations are true in both continuous energy space and also in a constant cross section world. Equation (1) is true at all energies. Equation (2) is true for all 1/v capture cross sections. So, any approximations in equations (4), (5), and (6) must be due to the approximations made in equation (3) for the number of collisions.

The assumption that is made in equation (3) is that the average of the scattering ratio (SR) is the same as the flux weighted average of scattering cross section divided by the flux weighted average of the total cross section. Since the scatter and total cross sections are highly correlated, the approximation is very good.

In effect, an MCNP calculation uses the average of the scattering ratio, while formulas (4), (5), and (6) use the separate averages for the scattering and total cross sections.

Neutron lifetimes can be read directly off of the MCNP outputs from the calculations of the test problems. The number of collisions (be sure implicit capture is turned off) is also a simple MCNP table edit.

Using the results from the MCNP calculations of the sample problems, the average neutron velocity is the ratio of the F4 flux tally / the inverse velocity weighted flux tally (F14 in the sample deck). Note that at room temperature, the well-known 2200 m/sec is a most likely velocity, whereas this procedure gives the Maxwellian average velocity of 2482 m/sec. The difference between them is a factor of 2/sqrt(π).

Flux weighted cross sections are the ratio of the cross section multiplied flux tallies (F24 in the sample input deck) and the F4 flux tally.

The averaged cross sections calculated from equations (4), (5), and (6) match the flux averaged cross sections very, very closely for all materials, all temperatures, and both scattering treatments. The only differences of 1 or 2 % occur occasionally in the free gas materials containing U-238 and its 6.7 eV resonance.

Some sample scattering results are given below:

Table 4: Estimated and Actual Averaged Scattering Cross Sections for H_2O.

H_2O S(α,β)	temp (MeV)	temp (K)	avg. no. collisions	estimated avg. scatter xs (b)	flux weighted scatter xs (b)
	2.444E-08	283.61	161.37	32.0607	32.0615
	2.530E-08	293.59	162.54	31.7383	31.7382
	2.585E-08	299.98	163.22	31.5350	31.5346
	2.789E-08	323.65	165.81	30.8464	30.8468
	3.016E-08	349.99	168.66	30.1739	30.1742
	3.219E-08	373.55	171.09	29.6267	29.6274
	3.447E-08	400.01	173.72	29.0759	29.0760
	3.650E-08	423.57	176.08	28.6412	28.6418
	3.878E-08	450.02	178.66	28.1933	28.1944
	4.081E-08	473.58	180.97	27.8422	27.8421
	4.309E-08	500.04	183.59	27.4913	27.4928
	4.512E-08	523.60	185.81	27.1897	27.1912
	4.740E-08	550.05	188.35	26.8937	26.8938
	4.943E-08	573.61	190.45	26.6284	26.6289
	5.170E-08	599.95	192.75	26.3519	26.3533
	5.374E-08	623.63	194.92	26.1397	26.1404
	5.601E-08	649.97	197.19	25.9053	25.9047
	6.894E-08	800.02	210.79	24.9680	24.9680

Table 5: Estimated and Actual Averaged Scattering Cross Sections for rgraphite10.

grph10 S(α,β)	temp (MeV)	temp (K)	avg. no. collisions	estimated scatter xs (b)	flux weighted scatter xs (b)
	2.551E-08	296	1412.4	4.9414	4.9423
	3.447E-08	400	1653.9	4.9441	4.9438
	4.309E-08	500	1854.7	4.9437	4.9438
	5.170E-08	600	2036.5	4.9439	4.9438
	6.032E-08	700	2202.7	4.9443	4.9438
	6.894E-08	800	2357.6	4.9439	4.9440
	8.617E-08	1000	2640.1	4.9396	4.9435
	1.034E-07	1200	2894.4	4.9440	4.9439
	1.379E-07	1600	3348.6	4.9438	4.9439
	1.723E-07	2000	3748.6	4.9444	4.9438

Table 6: Estimated and Actual Averaged Scattering Cross Sections for UO_2.

UO_2 S(α,β)	temp (MeV)	temp (K)	avg. no. collisions	estimated scatter xs (b)	flux weighted scatter xs (b)
	2.551E-08	296	11.25	8.1118	8.1126
	3.447E-08	400	12.49	7.8334	7.8348
	4.309E-08	500	13.34	7.5428	7.5442
.	5.170E-08	600	14.01	7.2726	7.2736
	6.032E-08	700	14.57	7.0352	7.0371
	6.894E-08	800	15.08	6.8374	6.8377
	8.617E-08	1000	15.97	6.5329	6.5340
	1.034E-07	1200	16.81	6.3252	6.3263

Note that the average neutron velocity (and the flux weighted cross sections) are obtained by a ratio of two random quantities. The ratio of two independent random variables is a biased estimator, but in this case, the numerator and denominator terms are very highly correlated on a very fine energy grid. They are both calculated from the same track length path with only a very small change in the inverse velocity (or cross section) within each fine energy grid interval of the numerator. Working with these fine energy grid ratios can be interpreted as a discrete (i.e., a fine energy grid) approximation to a continuous flux-weighted integral over energy to calculate an averaged quantity.

Alternatively, if the total cross section is known as a function of energy, then En and EMn cards on a fine energy grid can be used to average the inverse of the total cross section.

The mfp edit given by MCNP can be calculated with MCNP tallies on this kind of fine energy grid mesh. First, calculate the flux weighted total cross section on a fine grid energy mesh. Next,

convert the tally fine energy grid total cross section values into mean free paths. Finally, manually (or in a spreadsheet) flux-weight the fine energy grid mfp's and divide by the integrated F4 flux. So, the mfp edit in MCNP is simply a flux-weighted average mfp and would correspond to flux-weighting the inverse of the total cross section.

As such, the inverse of the mfp given by MCNP can be seen as the harmonic mean of the total cross section corresponding to the arithmetic mean of the flux weighted total cross section. The harmonic mean is always slightly smaller than the arithmetic mean.

The averaged neutron velocity calculated from the inverse velocity weighted flux tally is also a harmonic mean and is thus always somewhat smaller than an arithmetic mean of the neutron velocity. The arithmetic mean of the velocity can be calculated using a fine energy grid on the flux tallies (En) and putting appropriate averaged velocities on that grid using an energy multiplier (EMn) card.

IX. Observations from the Tabulated MCNP Results Using the Re-Released Data

The tsl materials containing H (with its ~20 b scattering cross section and low atomic weight and high number density) have the shortest mfp's. The shortest lifetimes and fewest number of collisions come from tsl materials with significant capture cross sections (see especially Al, Fe, UN, and UO_2). The number of collisions is inversely related to the capture cross section. The most collisions occur in D_2O, which has almost no capture cross section.

Temperature effects for thermal scattering can be studied by changing the material temperature (and the fixed neutron source temperature). Values for the ZAID suffixes of the cross section and S(α,β) material should also be made consistent with the desired material temperature. For simplicity and consistency, a constant density is assumed for the scattering material at various temperatures. As the temperature increases, the number of collisions and the average neutron velocity increase. For S(α,β) materials, the mfp goes up (ie the cross section goes down) with respect to temperature, while for free gas materials, the mfp is relatively constant with respect to temperature. As the temperature increases, the S(α,β) results should begin to approach the free gas results for the same material.

The effects of the tsl versus free gas modelling can be seen by either including the tsl material MTm card or not including the material MTm card. The difference between the S(α,β) and the free gas results is a good indication of how important (or unimportant) the thermal scattering effects are. SiC and SiO_2 do not show much difference between the S(α,β) and the free gas results.

A neutron energy spectrum can be obtained with a fine energy grid on the F4 flux tally. The shape of this spectrum will be roughly similar to a Maxwellian shape. The difference comes from the (presumably small) 1/v capture cross section that is present in the scattering material. Flux spectrum plots are given for room temperature H_2O and D_2O in Figures 16 and 17.

For the two cases involving U-238, (UN and UO_2), and also the cases with Al and Fe, the capture cross section is roughly 10% of the total cross section and the number of collisions per history are quite small compared to the other TSL materials. Thus, these four flux distributions are not very much like a Maxwellian distribution. Furthermore, U-238 has a big resonance at 6.7 eV which changes the shape of the capture cross section away from the usual 1/v shape for UN and UO_2.

Tabular and graphical results follow in the next section which document these observations. Note that although MCNP only gives relative errors on the tally results (typically << 0.1 %), an approximate idea of the relative error in the other results (mfp, collisions, lifetimes) can be seen in the constancy of the lifetime results (the neutron lifetimes are theoretically independent of temperature for 1/v (or nearly 1/v) cross sections). With the very large number (10 million) of histories employed here, the statistical error is very small. Using the standard rule for Monte Carlo estimates (1/sqrt(number of histories)), and knowing that all particle histories contribute to the quantities of interest, there should be 3 to 4 places of precision in all of the MCNP produced results.

X. Tabulated and Graphical Results from the MCNP Test Problems

Table 7: Temperature Effects due to the S(α,β) cross sections for light water (constant density = 1.0 g/cc)

H_2O S(α,β)	temp (MeV)	temp (K)	avg. no. collisions	lifetime (sh)	mfp (cm)	avg n vel (m/sec)
	2.444E-08	283.6	161.37	2.0435E+04	0.3294	2440
	2.530E-08	293.6	162.54	2.0435E+04	0.3329	2483
	2.585E-08	300.0	163.22	2.0432E+04	0.3351	2510
	2.789E-08	323.7	165.81	2.0432E+04	0.3427	2607
	3.016E-08	350.0	168.66	2.0431E+04	0.3504	2711
	3.219E-08	373.5	171.09	2.0432E+04	0.3569	2801
	3.447E-08	400.0	173.72	2.0431E+04	0.3636	2899
	3.650E-08	423.6	176.08	2.0430E+04	0.3690	2983
	3.878E-08	450.0	178.66	2.0433E+04	0.3747	3074
	4.081E-08	473.6	180.97	2.0431E+04	0.3793	3154
	4.309E-08	500.0	183.59	2.0431E+04	0.3841	3241
	4.512E-08	523.6	185.81	2.0432E+04	0.3882	3316
	4.740E-08	550.1	188.35	2.0432E+04	0.3925	3399
	4.943E-08	573.6	190.45	2.0433E+04	0.3962	3471
	5.170E-08	600.0	192.75	2.0433E+04	0.4002	3550
	5.374E-08	623.6	194.92	2.0434E+04	0.4034	3619
	5.601E-08	650.0	197.19	2.0432E+04	0.4069	3695
	6.894E-08	800.0	210.79	2.0433E+04	0.4226	4099

Table 8: Temperature Effects due to the free gas cross sections for light water (constant density = 1.0 g/cc)

H_2O free	temp (MeV)	temp (K)	avg. no. collisions	lifetime (sh)	mfp (cm)	avg n vel (m/sec)
	2.444E-08	283.6	103.79	2.0424E+04	0.5023	2439
	2.530E-08	293.6	105.67	2.0423E+04	0.5023	2483
	2.585E-08	300.0	106.80	2.0424E+04	0.5024	2510
	2.789E-08	323.7	110.90	2.0425E+04	0.5026	2607
	3.016E-08	350.0	115.28	2.0423E+04	0.5027	2711
	3.219E-08	373.5	119.05	2.0422E+04	0.5028	2801
	3.447E-08	400.0	123.17	2.0423E+04	0.5030	2899
	3.650E-08	423.6	126.70	2.0421E+04	0.5031	2983
	3.878E-08	450.0	130.57	2.0421E+04	0.5032	3075
	4.081E-08	473.6	133.92	2.0422E+04	0.5033	3154

4.309E-08	500.0	137.58	2.0421E+04	0.5034	3241
4.512E-08	523.6	140.76	2.0421E+04	0.5035	3316
4.740E-08	550.1	144.24	2.0421E+04	0.5035	3399
4.943E-08	573.6	147.27	2.0419E+04	0.5036	3471
5.170E-08	600.0	150.61	2.0422E+04	0.5037	3550
5.374E-08	623.6	153.53	2.0422E+04	0.5037	3619
5.601E-08	650.0	156.71	2.0421E+04	0.5038	3695
6.894E-08	800.0	173.77	2.0423E+04	0.5041	4099

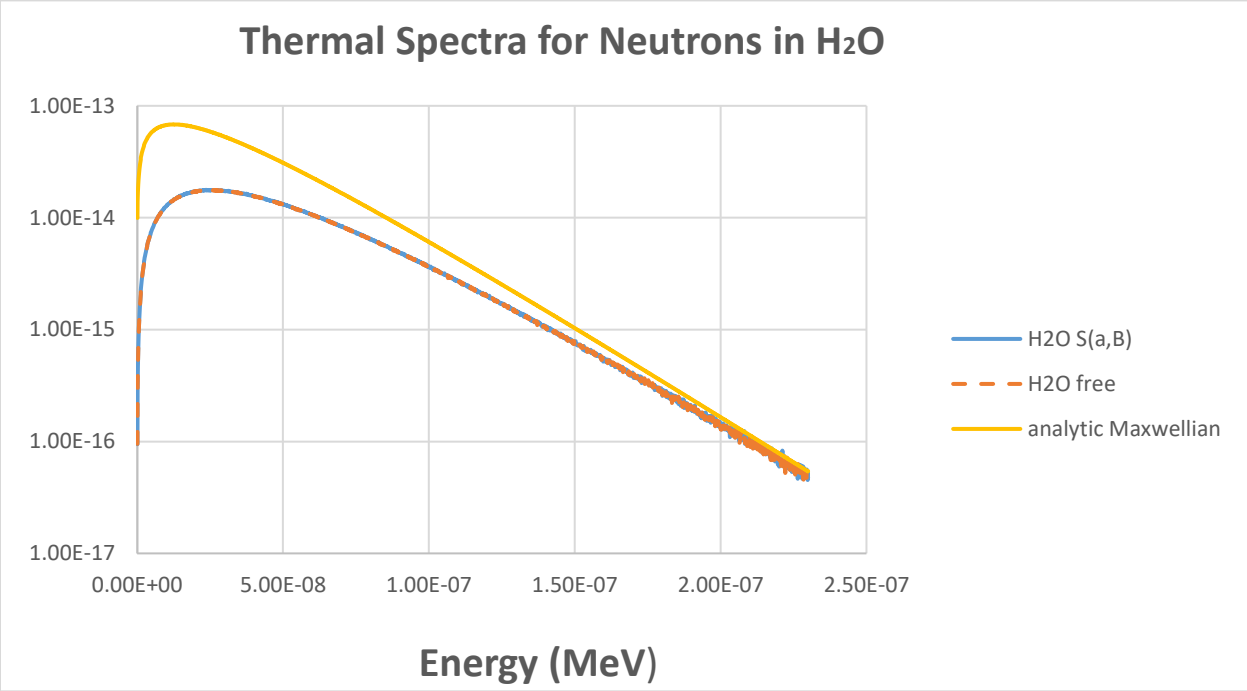

Figure 16: Thermal Neutron Spectra in Room Temperature Light Water

Table 9: Temperature Effects due to the S(α,β) cross sections for heavy water (constant density = 1.1 g/cc)

D_2O S(α,β)	temp (MeV)	temp (K)	avg. no. collisions	lifetime (sh)	mfp (cm)	avg n vel (m/sec)
	2.44E-08	284	13112	1.16E+07	2.1982	2441
	2.53E-08	294	13313	1.16E+07	2.2036	2483
	2.59E-08	300	13428	1.16E+07	2.2082	2510
	2.79E-08	324	13847	1.16E+07	2.2241	2607
	3.11E-08	360	14322	1.16E+07	2.2376	2711
	3.22E-08	374	14717	1.16E+07	2.2511	2801
	3.45E-08	400	15159	1.16E+07	2.2626	2899
	3.65E-08	424	15539	1.16E+07	2.2710	2983
	3.88E-08	450	15947	1.16E+07	2.2810	3074
	4.08E-08	474	16290	1.16E+07	2.2905	3154
	4.31E-08	500	16714	1.16E+07	2.2957	3241
	4.51E-08	524	17087	1.16E+07	2.2995	3316
	4.74E-08	550	17490	1.16E+07	2.3041	3399
	4.94E-08	574	17882	1.16E+07	2.3044	3471
	5.17E-08	600	18327	1.16E+07	2.3029	3550
	5.37E-08	624	18714	1.16E+07	2.3014	3619
	5.60E-08	650	19135	1.16E+07	2.3012	3695

Table 10: Temperature Effects due to the free gas cross sections for heavy water (constant density = 1.1 g/cc)

D_2O Free	temp (MeV)	temp (K)	avg. no. collisions	lifetime (sh)	mfp (cm)	avg n vel (m/sec)
	2.444E-08	283.6	11464	1.1619E+07	2.5102	2438
	2.530E-08	293.6	11659	1.1620E+07	2.5105	2482
	2.585E-08	300.0	11785	1.1621E+07	2.5108	2509
	2.789E-08	323.7	12243	1.1623E+07	2.5106	2606
	3.106E-08	360.4	12753	1.1627E+07	2.5105	2710
	3.219E-08	373.5	13153	1.1626E+07	2.5105	2800
	3.447E-08	400.0	13615	1.1625E+07	2.5105	2898
	3.650E-08	423.6	14008	1.1623E+07	2.5105	2982
	3.878E-08	450.0	14448	1.1626E+07	2.5106	3073
	4.081E-08	473.6	14817	1.1627E+07	2.5106	3153
	4.309E-08	500.0	15215	1.1626E+07	2.5105	3240
	4.512E-08	523.6	15573	1.1626E+07	2.5105	3315
	4.740E-08	550.1	15974	1.1624E+07	2.5104	3398

4.943E-08	573.6	16314	1.1626E+07	2.5102	3470
5.170E-08	600.0	16683	1.1627E+07	2.5105	3549
5.374E-08	623.6	17004	1.1624E+07	2.5109	3618
5.601E-08	650.0	17358	1.1624E+07	2.5108	3694

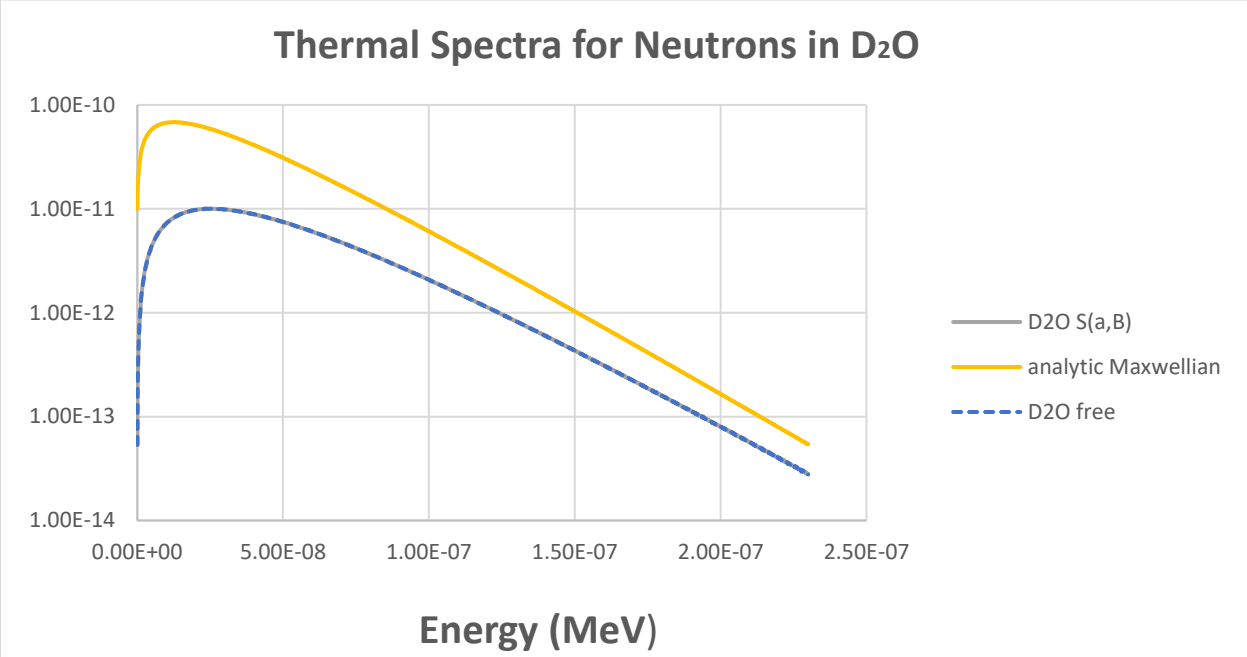

Figure 17: Thermal Neutron Spectra in Room Temperature Heavy Water

Table 11: Temperature Effects due to the S(α,β) cross sections for crystalline graphite (constant density = 2.2 g/cc)

cgrph S(α,β)	temp (MeV)	temp (K)	avg. no. collisions	lifetime (sh)	mfp (cm)	avg n vel (m/sec)
	2.551E-08	296	1414.6	1.0659E+06	1.9543	2494
	3.447E-08	400	1656.0	1.0662E+06	1.8918	2899
	4.309E-08	500	1856.1	1.0660E+06	1.8730	3241
	5.170E-08	600	2037.0	1.0665E+06	1.8652	3551
	6.032E-08	700	2201.5	1.0662E+06	1.8613	3835
	6.894E-08	800	2353.8	1.0656E+06	1.8590	4100
	8.617E-08	1000	2663.7	1.0653E+06	1.8564	4584
	1.034E-07	1200	2888.8	1.0658E+06	1.8548	5021
	1.379E-07	1600	3341.8	1.0661E+06	1.8524	5798
	1.723E-07	2000	3740.2	1.0660E+06	1.8507	6482

Table 12: Temperature Effects due to the free gas cross sections for crystalline graphite (constant density = 2.2 g/cc)

cgrph free	temp (MeV)	temp (K)	avg. no. collisions	lifetime (sh)	mfp (cm)	avg n vel (m/sec)
	2.551E-08	296	1450.4	1.0659E+06	1.8363	2493
	3.447E-08	400	1687.0	1.0660E+06	1.8359	2898
	4.309E-08	500	1885.8	1.0659E+06	1.8360	3240
	5.170E-08	600	2065.6	1.0659E+06	1.8361	3549
	6.032E-08	700	2231.2	1.0660E+06	1.8362	3833
	6.894E-08	800	2385.5	1.0661E+06	1.8362	4098
	8.617E-08	1000	2666.4	1.0659E+06	1.8364	4581
	1.034E-07	1200	2921.0	1.0660E+06	1.8364	5018
	1.379E-07	1600	3372.6	1.0658E+06	1.8364	5795
	1.723E-07	2000	3770.3	1.0659E+06	1.8365	6478

Table 13: Temperature Effects due to the S(α,β) cross sections for 10% porosity graphite (constant density = 2.0 g/cc)

grph10 S(α,β)	temp (MeV)	temp (K)	avg. no. collisions	lifetime (sh)	mfp (cm)	avg n vel (m/sec)
	2.551E-08	296	1412.4	1.1730E+06	2.1149	2494
	3.447E-08	400	1653.9	1.1726E+06	2.0697	2899
	4.309E-08	500	1854.7	1.1719E+06	2.0543	3241
	5.170E-08	600	2036.5	1.1724E+06	2.0472	3551
	6.032E-08	700	2202.7	1.1724E+06	2.0433	3835
	6.894E-08	800	2357.6	1.1726E+06	2.0408	4099
	8.617E-08	1000	2640.1	1.1727E+06	2.0379	4583
	1.034E-07	1200	2894.4	1.1723E+06	2.0360	5021
	1.379E-07	1600	3348.6	1.1725E+06	2.0333	5797
	1.723E-07	2000	3748.6	1.1727E+06	2.0317	6482

Table 14: Temperature Effects due to the free gas cross sections for 10% porosity graphite (constant density = 2.0 g/cc)

grph10 free	temp (MeV)	temp (K)	avg. no. collisions	lifetime (sh)	mfp (cm)	avg n vel (m/sec)
	2.551E-08	296	1450.4	1.1724E+06	2.0199	2493
	3.447E-08	400	1687.0	1.1726E+06	2.0195	2898
	4.309E-08	500	1885.8	1.1725E+06	2.0196	3240
	5.170E-08	600	2065.6	1.1725E+06	2.0197	3549
	6.032E-08	700	2231.2	1.1725E+06	2.0198	3833
	6.894E-08	800	2385.5	1.1727E+06	2.0198	4098
	8.617E-08	1000	2666.4	1.1735E+06	2.0201	4581
	1.034E-07	1200	2921.0	1.1725E+06	2.0200	5019
	1.379E-07	1600	3372.6	1.1724E+06	2.0201	5796
	1.723E-07	2000	3770.3	1.1725E+06	2.0201	6478

Table 15: Temperature Effects due to the S(α,β) cross sections for 30% porosity graphite (constant density = 1.6 g/cc)

grph30 S(α,β)	temp (MeV)	temp (K)	avg. no. collisions	lifetime (sh)	mfp (cm)	avg n vel (m/sec)
	2.551E-08	296	1400.4	1.4663E+06	2.6564	2494
	3.447E-08	400	1641.0	1.4655E+06	2.6032	2899
	4.309E-08	500	1844.1	1.4662E+06	2.5831	3241
	5.170E-08	600	2025.0	1.4655E+06	2.5726	3550
	6.032E-08	700	2192.2	1.4656E+06	2.5660	3835
	6.894E-08	800	2348.5	1.4656E+06	2.5615	4099
	8.617E-08	1000	2631.6	1.4657E+06	2.5553	4583
	1.034E-07	1200	2888.1	1.4657E+06	2.5511	5021
	1.379E-07	1600	3344.5	1.4661E+06	2.5426	5797
	1.723E-07	2000	3743.4	1.4653E+06	2.5422	6482

Table 16: Temperature Effects due to the free gas cross sections for 30% porosity graphite (constant density = 1.6 g/cc)

grph30 free	temp (MeV)	temp (K)	avg. no. collisions	lifetime (sh)	mfp (cm)	avg n vel (m/sec)
	2.551E-08	296	1450.4	1.4655E+06	2.5248	2493
	3.447E-08	400	1687.0	1.4658E+06	2.5244	2898
	4.309E-08	500	1885.8	1.4656E+06	2.5246	3240
	5.170E-08	600	2065.6	1.4656E+06	2.5247	3549
	6.032E-08	700	2231.2	1.4657E+06	2.5248	3833
	6.894E-08	800	2385.5	1.4658E+06	2.5247	4098
	8.617E-08	1000	2666.4	1.4656E+06	2.5251	4581
	1.034E-07	1200	2921.0	1.4657E+06	2.5250	5019
	1.379E-07	1600	3372.6	1.4655E+06	2.5251	5796
	1.723E-07	2000	3770.3	1.4657E+06	2.5252	6478

Table 17: Temperature Effects due to the S(α,β) cross sections for SiO_2 (constant density = 2.65 g/cc)

SiO_2 S(α,β)	temp (MeV)	temp (K)	avg. no. collisions	lifetime (sh)	mfp (cm)	avg n vel (m/sec)
	2.530E-08	294	63.423	1.0078E+05	3.985	2484
	3.016E-08	350	69.836	1.0085E+05	3.939	2712
	3.447E-08	400	74.919	1.0080E+05	3.915	2899
	4.309E-08	500	84.041	1.0073E+05	3.892	3241
	6.894E-08	800	106.55	1.0074E+05	3.878	4100
	8.617E-08	1000	118.91	1.0068E+05	3.884	4584
	9.479E-08	1100	124.92	1.0076E+05	3.880	4808

Table 18: Temperature Effects due to the free gas cross sections for SiO_2 (constant density = 2.65 g/cc)

SiO_2 free gas	temp (MeV)	temp (K)	avg. no. collisions	lifetime (sh)	mfp (cm)	avg n vel (m/sec)
	2.530E-08	294	66.33	1.0076E+05	3.778	2483
	3.016E-08	350	72.33	1.0076E+05	3.783	2710
	3.447E-08	400	77.27	1.0077E+05	3.786	2898
	4.309E-08	500	86.28	1.0078E+05	3.791	3240
	6.894E-08	800	108.91	1.0081E+05	3.800	4098
	8.617E-08	1000	121.63	1.0081E+05	3.804	4582
	9.479E-08	1100	127.51	1.0081E+05	3.805	4805

Table 19: Temperature Effects due to the S(α,β) cross sections for H in CH_2 (poly) (constant density = 0.92 g/cc)

h-poly S(α,β)	temp (MeV)	temp (K)	avg. no. collisions	lifetime (sh)	mfp (cm)	avg n vel (m/sec)
	6.635E-09	77	121.19	1.7180E+04	0.1830	1272
	1.689E-08	196	161.82	1.7190E+04	0.2249	2029
	2.008E-08	233	168.88	1.7185E+04	0.2367	2213
	2.530E-08	294	178.02	1.7188E+04	0.2548	2483
	2.585E-08	300	178.85	1.7189E+04	0.2566	2510
	2.611E-08	303	179.25	1.7191E+04	0.2575	2522
	2.697E-08	313	180.51	1.7192E+04	0.2603	2564
	2.783E-08	323	181.72	1.7193E+04	0.2630	2604
	2.870E-08	333	182.85	1.7189E+04	0.2657	2645
	2.956E-08	343	183.99	1.7190E+04	0.2683	2684
	3.016E-08	350	184.71	1.7185E+04	0.2701	2711

Table 20: Temperature Effects due to the free gas cross sections for H in CH_2 (poly) (constant density = 0.92 g/cc)

h-poly free	temp (MeV)	temp (K)	avg. no. collisions	lifetime (sh)	mfp (cm)	avg n vel (m/sec)
	6.635E-09	77	55.17	1.7170E+04	0.4142	1272
	1.689E-08	196	87.46	1.7178E+04	0.4168	2029
	2.008E-08	233	95.29	1.7181E+04	0.4172	2213
	2.530E-08	294	106.84	1.7181E+04	0.4176	2484
	2.585E-08	300	107.98	1.7182E+04	0.4177	2510
	2.611E-08	303	108.51	1.7181E+04	0.4177	2523
	2.697E-08	313	110.26	1.7179E+04	0.4177	2564
	2.783E-08	323	111.99	1.7179E+04	0.4178	2605
	2.870E-08	333	113.71	1.7179E+04	0.4178	2645
	2.956E-08	343	115.38	1.7178E+04	0.4179	2684
	3.016E-08	350	116.53	1.7178E+04	0.4179	2712

Table 21: Temperature Effects due to the S(α,β) cross sections for Be (constant density = 1.85 g/cc)

Be S(α,β)	temp (MeV)	temp (K)	avg. no. collisions	lifetime (sh)	mfp (cm)	avg n vel (m/sec)
	2.551E-08	296	682.2	3.6658E+05	1.6406	2494
	3.447E-08	400	805.9	3.6672E+05	1.4041	2899
	4.309E-08	500	909.1	3.6660E+05	1.3409	3241
	5.170E-08	600	1002.1	3.6651E+05	1.3148	3551
	6.032E-08	700	1087.3	3.6636E+05	1.3012	3835
	6.894E-08	800	1166.4	3.6624E+05	1.2930	4100
	8.617E-08	1000	1311.6	3.6627E+05	1.2833	4584
	1.034E-07	1200	1442.9	3.6637E+05	1.2777	5021

Table 22: Temperature Effects due to the free gas cross sections for Be (constant density = 1.85 g/cc)

Be free	temp (MeV)	temp (K)	avg. no. collisions	lifetime (sh)	mfp (cm)	avg n vel (m/sec)
	2.551E-08	296	733.9	3.6675E+05	1.2504	2492
	3.447E-08	400	853.3	3.6665E+05	1.2502	2898
	4.309E-08	500	953.8	3.6661E+05	1.2504	3240
	5.170E-08	600	1044.7	3.6661E+05	1.2505	3549
	6.032E-08	700	1128.0	3.6652E+05	1.2506	3833
	6.894E-08	800	1205.5	3.6640E+05	1.2506	4098
	8.617E-08	1000	1347.3	3.6632E+05	1.2508	4582
	1.034E-07	1200	1476.0	3.6638E+05	1.2508	5019

Table 23: Temperature Effects due to the S(α,β) cross sections for BeO (constant density = 2.96 g/cc)

BeO S(α,β)	temp (MeV)	temp (K)	avg. no. collisions	lifetime (sh)	mfp (cm)	avg n vel (m/sec)
	2.530E-08	294	1078.5	6.2473E+05	1.7039	2483
	3.447E-08	400	1278.6	6.2499E+05	1.4888	2898
	4.309E-08	500	1438.5	6.2459E+05	1.4360	3240
	5.170E-08	600	1582.8	6.2442E+05	1.4145	3550
	6.032E-08	700	1716.9	6.2483E+05	1.4032	3834
	6.894E-08	800	1840.5	6.2465E+05	1.3961	4099
	8.617E-08	1000	2068.1	6.2470E+05	1.3870	4584
	1.034E-07	1200	2273.2	6.2428E+05	1.3808	5021

Table 24: Temperature Effects due to the free gas cross sections for BeO (constant density = 2.96 g/cc)

BeO free	temp (MeV)	temp (K)	avg. no. collisions	lifetime (sh)	mfp (cm)	avg n vel (m/sec)
	2.530E-08	294	1151.5	6.2510E+05	1.3518	2483
	3.447E-08	400	1343.2	6.2478E+05	1.3520	2898
	4.309E-08	500	1501.3	6.2462E+05	1.3521	3240
	5.170E-08	600	1644.2	6.2455E+05	1.3522	3549
	6.032E-08	700	1775.2	6.2430E+05	1.3522	3833
	6.894E-08	800	1897.8	6.2432E+05	1.3522	4098
	8.617E-08	1000	2121.6	6.2433E+05	1.3524	4582
	1.034E-07	1200	2323.7	6.2423E+05	1.3524	5019

Table 25: Temperature Effects due to the S(α,β) cross sections for ZrH (constant density = 5.56 g/cc)

ZrH S(α,β)	temp (MeV)	temp (K)	avg. no. collisions	lifetime (sh)	mfp (cm)	avg n vel (m/sec)
	2.551E-08	296	178.12	3.6003E+04	0.5469	2493
	3.447E-08	400	187.24	3.6009E+04	0.6114	2898
	4.309E-08	500	195.02	3.5976E+04	0.6562	3240
	5.170E-08	600	203.10	3.5991E+04	0.6881	3549
	6.032E-08	700	211.25	3.5989E+04	0.7110	3833
	6.894E-08	800	219.56	3.5994E+04	0.7278	4098
	8.617E-08	1000	236.16	3.5995E+04	0.7498	4582
	1.034E-07	1200	252.47	3.5990E+04	0.7629	5019

Table 26: Temperature Effects due to the free gas cross sections for ZrH (constant density = 5.56 g/cc)

ZrH free	temp (MeV)	temp (K)	avg. no. collisions	lifetime (sh)	mfp (cm)	avg n vel (m/sec)
	2.551E-08	296	113.83	3.5992E+04	0.8185	2493
	3.447E-08	400	132.39	3.5988E+04	0.8184	2899
	4.309E-08	500	147.93	3.5992E+04	0.8189	3241
	5.170E-08	600	161.91	3.5986E+04	0.8194	3550
	6.032E-08	700	174.80	3.5988E+04	0.8198	3835
	6.894E-08	800	186.86	3.5993E+04	0.8200	4099
	8.617E-08	1000	208.74	3.5989E+04	0.8205	4583
	1.034E-07	1200	228.56	3.5985E+04	0.8207	5021

Table 27: Temperature Effects due to the S(α,β) cross sections for SiC (constant density = 3.21 g/cc)

SiC S(α,β)	temp (MeV)	temp (K)	avg. no. collisions	lifetime (sh)	mfp (cm)	avg n vel (m/sec)
	2.585E-08	300	45.71	5.4340E+04	3.0282	2510
	3.447E-08	400	53.04	5.4351E+04	2.9937	2899
	4.309E-08	500	59.44	5.4342E+04	2.9772	3241
	5.170E-08	600	65.24	5.4369E+04	2.9679	3550
	6.032E-08	700	70.52	5.4348E+04	2.9621	3835
	6.894E-08	800	75.44	5.4336E+04	2.9584	4100
	8.617E-08	1000	84.44	5.4334E+04	2.9540	4584
	1.034E-07	1200	92.57	5.4345E+04	2.9519	5022

Table 28: Temperature Effects due to the free gas cross sections for SiC (constant density = 3.21 g/cc)

SiC free	temp (MeV)	temp (K)	avg. no. collisions	lifetime (sh)	mfp (cm)	avg n vel (m/sec)
	2.585E-08	300	46.73	5.4357E+04	2.9273	2510
	3.447E-08	400	53.80	5.4345E+04	2.9345	2898
	4.309E-08	500	60.02	5.4332E+04	2.9399	3240
	5.170E-08	600	65.65	5.4331E+04	2.9441	3549
	6.032E-08	700	70.85	5.4343E+04	2.9473	3833
	6.894E-08	800	75.68	5.4349E+04	2.9496	4098
	8.617E-08	1000	84.50	5.4356E+04	2.9543	4582
	1.034E-07	1200	92.48	5.4362E+04	2.9568	5019

Table 29: Temperature Effects due to the S(α,β) cross sections for YH_2 (constant density = 4.45 g/cc)

YH_2 S(α,β)	temp (MeV)	temp (K)	avg. no. collisions	lifetime (sh)	mfp (cm)	avg n vel (m/sec)
	2.530E-08	294	58.48	7.9393E+03	0.3708	2480
	3.447E-08	400	61.24	7.9351E+03	0.4165	2894
	4.309E-08	500	63.84	7.9379E+03	0.4460	3235
	5.170E-08	600	66.51	7.9384E+03	0.4664	3545
	6.032E-08	700	69.27	7.9384E+03	0.4807	3829
	6.894E-08	800	72.09	7.9406E+03	0.4911	4093
	8.617E-08	1000	77.66	7.9377E+03	0.5045	4577
	1.034E-07	1200	83.18	7.9419E+03	0.5126	5015
	1.206E-07	1400	88.47	7.9420E+03	0.5179	5417
	1.379E-07	1600	93.62	7.9457E+03	0.5215	5793

Table 30: Temperature Effects due to the free gas cross sections for YH_2 (constant density = 4.45 g/cc)

YH_2 free	temp (MeV)	temp (K)	avg. no. collisions	lifetime (sh)	mfp (cm)	avg n vel (m/sec)
	2.530E-08	294	39.05	7.9318E+03	0.5261	2483
	3.447E-08	400	45.42	7.9329E+03	0.5279	2899
	4.309E-08	500	50.68	7.9347E+03	0.5290	3241
	5.170E-08	600	55.41	7.9345E+03	0.5298	3550
	6.032E-08	700	59.78	7.9361E+03	0.5305	3835
	6.894E-08	800	63.85	7.9364E+03	0.5310	4099
	8.617E-08	1000	71.27	7.9373E+03	0.5319	4583
	1.034E-07	1200	78.00	7.9394E+03	0.5325	5021
	1.206E-07	1400	84.16	7.9408E+03	0.5330	5422
	1.379E-07	1600	89.94	7.9419E+03	0.5333	5798

Table 31: Temperature Effects due to the S(α,β) cross sections for UN (constant density = 11.0 g/cc)

UN S(α,β)	temp (MeV)	temp (K)	avg. no. collisions	lifetime (sh)	mfp (cm)	avg n vel (m/sec)
	2.551E-08	296	5.58	3.7693E+03	1.6947	2492
	3.447E-08	400	6.39	3.7663E+03	1.7152	2897
	4.309E-08	500	7.07	3.7630E+03	1.7306	3238
	5.170E-08	600	7.67	3.7580E+03	1.7430	3546
	6.032E-08	700	8.23	3.7558E+03	1.7534	3830
	6.894E-08	800	8.74	3.7507E+03	1.7622	4093
	8.617E-08	1000	9.67	3.7439E+03	1.7766	4575
	1.034E-07	1200	10.50	3.7359E+03	1.7879	5010

Table 32: Temperature Effects due to the free gas cross sections for UN (constant density = 11.0 g/cc)

UN free	temp (MeV)	temp (K)	avg. no. collisions	lifetime (sh)	mfp (cm)	avg n vel (m/sec)
	2.551E-08	296	5.81	3.8513E+03	1.6310	2492
	3.447E-08	400	6.59	3.8472E+03	1.6687	2896
	4.309E-08	500	7.24	3.7686E+03	1.6938	3238
	5.170E-08	600	7.82	3.7648E+03	1.7134	3546
	6.032E-08	700	8.36	3.7612E+03	1.7290	3829
	6.894E-08	800	8.86	3.7518E+03	1.7414	4093
	8.617E-08	1000	9.76	3.7438E+03	1.7617	4574
	1.034E-07	1200	10.58	3.7357E+03	1.7765	5009

Table 33: Temperature Effects due to the S(α,β) cross sections for UO_2 (constant density = 11.0 g/cc)

UO_2 S(α,β)	temp (MeV)	temp (K)	avg. no. collisions	lifetime (sh)	mfp (cm)	avg n vel (m/sec)
	2.551E-08	296	11.25	6.8947E+03	1.5360	2491
	3.447E-08	400	12.49	6.8842E+03	1.6086	2894
	4.309E-08	500	13.34	6.8731E+03	1.6833	3235
	5.170E-08	600	14.01	6.8605E+03	1.7554	3542
	6.032E-08	700	14.57	6.8516E+03	1.8211	3826
	6.894E-08	800	15.08	6.8420E+03	1.8789	4089
	8.617E-08	1000	15.97	6.8174E+03	1.9722	4567
	1.034E-07	1200	16.81	6.7929E+03	2.0406	5000

Table 34: Temperature Effects due to the free gas cross sections for UO_2 (constant density = 11.0 g/cc)

UO_2 free	temp (MeV)	temp (K)	avg. no. collisions	lifetime (sh)	mfp (cm)	avg n vel (m/sec)
	2.551E-08	296	8.19	6.8948E+03	2.1090	2491
	3.447E-08	400	9.34	6.9089E+03	2.1437	2895
	4.309E-08	500	10.30	6.9024E+03	2.1664	3236
	5.170E-08	600	11.17	6.8916E+03	2.1842	3543
	6.032E-08	700	11.96	6.8807E+03	2.1984	3826
	6.894E-08	800	12.70	6.8695E+03	2.2092	4089
	8.617E-08	1000	14.02	6.8312E+03	2.2276	4569
	1.034E-07	1200	15.20	6.8268E+03	2.2406	5002

Table 35: Temperature Effects due to the S(α,β) cross sections for Ice (constant density = 0.92 g/cc)

Ice S(α,β)	temp (MeV)	temp (K)	avg. no. collisions	lifetime (sh)	mfp (cm)	avg n vel (m/sec)
	9.910E-09	115	134.11	2.2202E+04	0.2649	1554
	1.621E-08	188	152.77	2.2206E+04	0.3037	1988
	1.794E-08	208	156.52	2.2209E+04	0.3131	2091
	1.966E-08	228	159.97	2.2218E+04	0.3220	2189
	2.009E-08	233	160.81	2.2223E+04	0.3241	2213
	2.138E-08	248	163.09	2.2215E+04	0.3303	2283
	2.181E-08	253	163.76	2.2205E+04	0.3323	2306
	2.311E-08	268	165.98	2.2211E+04	0.3381	2373
	2.354E-08	273	166.62	2.2201E+04	0.3400	2395

Table 36: Temperature Effects due to the free gas cross sections for Ice (constant density = 0.92 g/cc)

Ice free	temp (MeV)	temp (K)	avg. no. collisions	lifetime (sh)	mfp (cm)	avg n vel (m/sec)
	9.910E-09	115	66.47	2.2186E+04	0.5432	1554
	1.621E-08	188	84.78	2.2198E+04	0.5448	1988
	1.794E-08	208	89.14	2.2198E+04	0.5451	2091
	1.966E-08	228	93.27	2.2198E+04	0.5454	2189
	2.009E-08	233	94.27	2.2198E+04	0.5454	2213
	2.138E-08	248	97.41	2.2200E+04	0.5449	2284
	2.181E-08	253	98.19	2.2201E+04	0.5457	2306
	2.311E-08	268	101.04	2.2201E+04	0.5458	2374
	2.354E-08	273	101.97	2.2200E+04	0.5458	2395

Table 37: Temperature Effects due to the S(α,β) cross sections for benzene (constant density = 0.8765 g/cc)

benzene S(α,β)	temp (MeV)	temp (K)	avg. no. collisions	lifetime (sh)	mfp (cm)	avg n vel (m/sec)
	2.551E-08	296	180.84	3.3299E+04	0.4874	2493
	3.016E-08	350	182.84	3.3300E+04	0.5300	2711
	3.447E-08	400	193.54	3.3301E+04	0.5338	2898
	3.878E-08	450	198.85	3.3300E+04	0.5522	3074
	4.309E-08	500	197.79	3.3301E+04	0.5889	3240
	5.170E-08	600	213.26	3.3296E+04	0.5954	3550
	6.894E-08	800	222.74	3.3295E+04	0.6598	4099
	8.617E-08	1000	246.62	3.3300E+04	0.6619	4583

Table 38: Temperature Effects due to the free gas cross sections for benzene (constant density = 0.8765 g/cc)

benzene free	temp (MeV)	temp (K)	avg. no. collisions	lifetime (sh)	mfp (cm)	avg n vel (m/sec)
	2.551E-08	296	114.75	3.3277E+04	0.7524	2493
	3.016E-08	350	124.92	3.3275E+04	0.7518	2712
	3.447E-08	400	133.48	3.3275E+04	0.7522	2899
	3.878E-08	450	141.52	3.3275E+04	0.7525	3075
	4.309E-08	500	149.13	3.3279E+04	0.7528	3241
	5.170E-08	600	163.24	3.3273E+04	0.7532	3550
	6.894E-08	800	188.34	3.3274E+04	0.7537	4100
	8.617E-08	1000	210.46	3.3276E+04	0.7541	4583

Table 39: Temperature Effects due to the S(α,β) cross sections for Al (constant density = 2.7 g/cc)

Al S(α,β)	temp (MeV)	temp (K)	avg. no. collisions	lifetime (sh)	mfp (cm)	avg n vel (m/sec)
	1.723E-09	20	1.60	3.230E+04	15.710	648
	6.894E-09	80	3.88	3.229E+04	11.514	1296
	2.530E-08	294	7.39	3.231E+04	10.927	2483
	3.447E-08	400	8.54	3.231E+04	11.008	2899
	5.170E-08	600	10.31	3.230E+04	11.152	3551
	6.894E-08	800	11.79	3.231E+04	11.255	4099

Table 40: Temperature Effects due to the free gas cross sections for Al (constant density = 2.7 g/cc)

Al free	temp (MeV)	temp (K)	avg. no. collisions	lifetime (sh)	mfp (cm)	avg n vel (m/sec)
	1.723E-09	20	2.83	3.230E+04	7.597	648
	6.894E-09	80	4.66	3.229E+04	9.095	1296
	2.530E-08	294	8.02	3.231E+04	10.067	2483
	3.447E-08	400	9.19	3.231E+04	10.241	2899
	5.170E-08	600	11.03	3.230E+04	10.439	3550
	6.894E-08	800	12.59	3.230E+04	10.559	4099

Table 41: Temperature Effects due to the S(α,β) cross sections for Fe (constant density = 7.87 g/cc)

Fe S(α,β)	temp (MeV)	temp (K)	avg. no. collisions	lifetime (sh)	mfp (cm)	avg n vel (m/sec)
	1.723E-09	20	1.32	2.0598E+03	1.204	648
	6.894E-09	80	3.14	2.0587E+03	0.926	1296
	2.530E-08	294	6.02	2.0590E+03	0.858	2483
	3.447E-08	400	6.96	2.0593E+03	0.863	2898
	5.170E-08	600	8.39	2.0598E+03	0.875	3550
	6.894E-08	800	9.57	2.0591E+03	0.885	4100

Table 42: Temperature Effects due to the free gas cross sections for Fe (constant density = 7.87 g/cc)

Fe free	temp (MeV)	temp (K)	avg. no. collisions	lifetime (sh)	mfp (cm)	avg n vel (m/sec)
	1.723E-09	20	2.38	2.0592E+03	0.581	648
	6.894E-09	80	3.76	2.0589E+03	0.722	1296
	2.530E-08	294	6.28	2.0599E+03	0.820	2483
	3.447E-08	400	7.17	2.0602E+03	0.838	2898
	5.170E-08	600	8.55	2.0600E+03	0.859	3549
	6.894E-08	800	9.72	2.0598E+03	0.871	4099

Table 43: MCNP S(α,β) Results for Materials with only 1 Temperature

S(α,β)	temp (MeV)	temp (K)	avg. no. collisions	lifetime (sh)	mfp (cm)	avg n vel (m/sec)
lucite	2.585E-08	300	180.80	2.3879E+04	0.3496	2510
s methane	1.896E-09	22	27.11	1.7370E+04	0.4389	680
l methane	8.617E-09	100	103.00	2.1454E+04	0.3115	1450
parah	1.723E-09	20	1.51	2.6596E+04	11.9380	648
parad	1.637E-09	19	900.39	1.8550E+07	17.2660	748
orthoh	1.723E-09	20	36.59	2.6601E+04	0.7033	886
orthod	1.637E-09	19	1638.80	1.8550E+07	7.8167	629

(These neutron velocities are suspect for parad and orthoh, perhaps there is a data problem.)

(Densities used for these materials were 1.18, 0.522, 0.42262, 0.086, 0.1624, 0.086, and 0.1624 g/cc, respectively.)

Table 44: Settings Used the Processing of para and ortho H and D

	eval file B(1)	eval file B(4)	eval file B(6)	njoy input natom	njoy input Emax	njoy output xs at 7 eV
parah	40.87268	7.59	2	2	7.59	20.6953
parad	6.79	7.59	2	2	7.59	3.3908
orthoh	40.87268	7.59	2	2	7.59	20.8454
orthod	6.79	7.59	2	2	7.59	3.3913

Table 45: MCNP Free Gas Results for Materials with only 1 Temperature

free	temp (MeV)	temp (K)	avg. no. collisions	lifetime (sh)	mfp (cm)	avg n vel (m/sec)
lucite	2.585E-08	300	113.22	2.3863E+04	0.5516	2510
s methane	1.896E-09	22	28.92	1.7373E+04	0.4290	680
l methane	8.617E-09	100	60.50	2.1449E+04	0.5390	1449
parah	1.723E-09	20	26.60	2.6595E+04	0.6827	648
parad	1.637E-09	19	2365.80	1.8544E+07	5.0804	631
orthoh	1.723E-09	20	26.60	2.6595E+04	0.6827	648
orthod	1.637E-09	19	2365.80	1.8544E+07	5.0804	631

XI Cross-comparing ACER and GROUPR Results for thermal cross sections

Another method of verification for the ACER produced thermal scattering cross section data is to compare the ACER continuous energy results with GROUPR multi-group results. The same sequence of NJOY processing is used for both sets of results. It is required that the same THERMR inputs are used for both. The part of the processing done in ACER along with the user input to ACER can thus be verified by comparison with the processing done in GROUPR along with the user input to GROUPR.

For the 3 kinds of thermal scattering law data (no elastic data, coherent elastic data, and incoherent elastic data), comparisons have been made between the results from ACER and GROUPR. For the GROUPR runs, a smooth weighting function was chosen with an arbitrary energy grid chosen to give a reasonable number of groups in the thermal energies up to Emax.

A typical GROUPR input file with 75 groups is given below. It is the reactor graphite at 400 K case. The associated THERMR input file is also given. The incoherent inelastic scattering is put into mt 221, and the coherent elastic scattering is put into mt 222. For this example, the GROUPR results are taken from the printed output file.

```
thermr
    30 -25 -26
    31 625 20 2 2 0 0 1 221 1 /
    400.0 500.0 /
    .001 10.00008/

…

groupr
    20 28 0 0 /
    625 1 0 2 4 1 1 1    /
    ' groupr run for tsl data '   /
    400.0       /
    1e10       /
    75
    1e-5 1.5e-5 2e-5 3e-5 4e-5 5e-5 6e-5 7e-5 8e-5 9e-5
    1e-4 1.5e-4 2e-4 3e-4 4e-4 5e-4 6e-4 7e-4 8e-4 9e-4
    1e-3 1.5e-3 2e-3 2.5e-3 3e-3 3.5e-3 4e-3 4.5e-3 5e-3
    5.5e-3 6e-3 6.5e-3 7e-3 7.5e-3 8e-3 8.5e-3 9e-3 9.5e-3
    1e-2 1.5e-2 2e-2 2.5e-2 3e-2 3.5e-2 4e-2 4.5e-2 5e-2
    5.5e-2 6e-2 6.5e-2 7e-2 7.5e-2 8e-2 8.5e-2 9e-2 9.5e-2
    1e-1 2e-1 3e-1 4e-1 5e-1 6e-1 7e-1 8e-1 9e-1
    1e-0 2e-0 3e-0 4e-0 5e-0 6e-0 7e-0 8e-0 9e-0
    1e+1 20e+6
    3   /
    3   221   /
    3   222   /
    6   /
    6   221   /
    6   222   /
  0 /
```

```
  0 /
stop
```

Typical results are given in Figures 18-20 for water (no elastic thermal scattering), graphite (coherent elastic), and H in ZrH (incoherent elastic) at different temperatures. All of the GROUPR results are shown as "stairsteps" coinciding with the energy group structure.

The agreement is very good. In fact, the H in ZrH comparison could have prevented 10 of the major problems encountered during the original release of the S(α,β) files. See Figure 21.

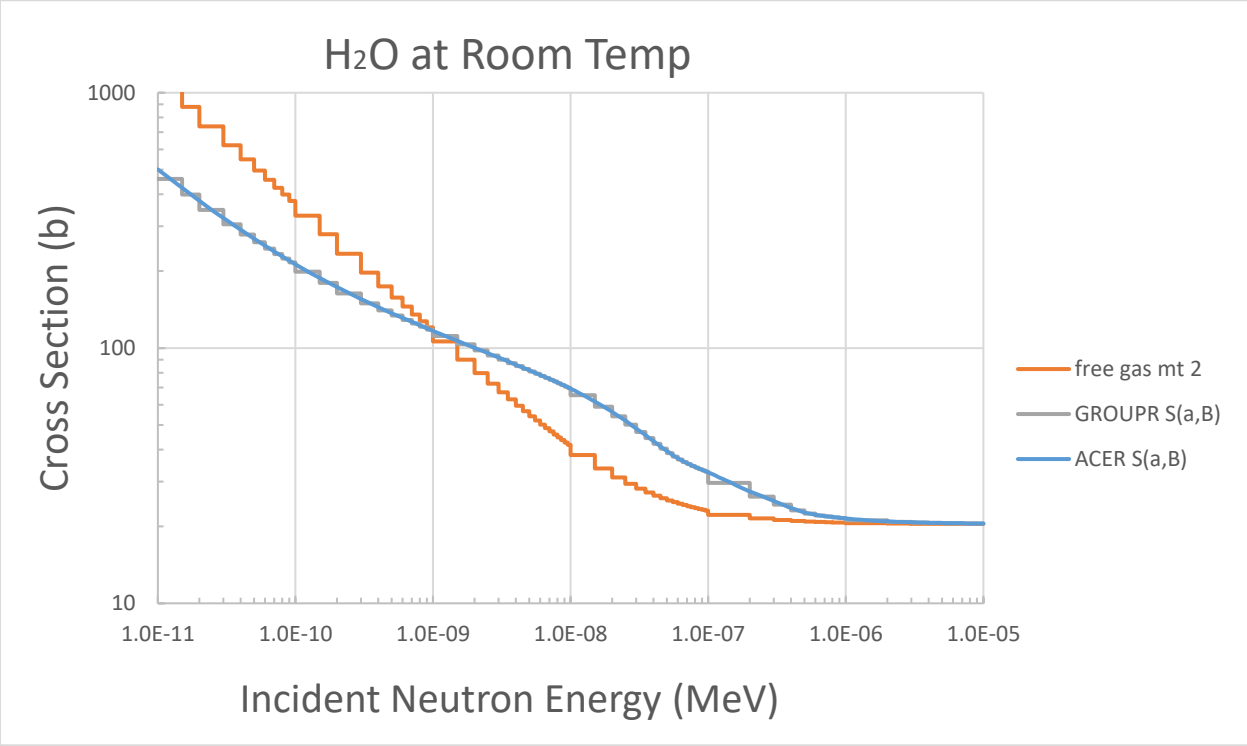

Figure 18: Comparison of ACER and GROUPR thermal scattering data for H_2O

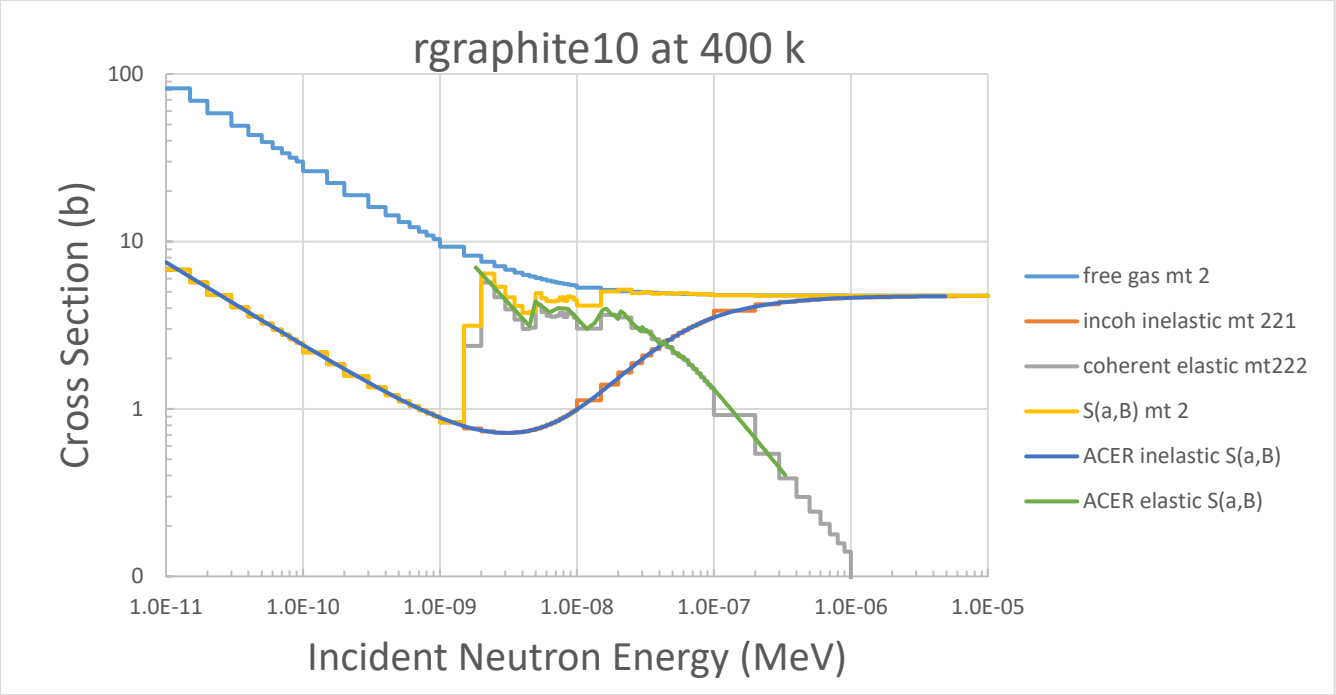

Figure 19: Comparison of ACER and GROUPR thermal scattering data for rgraphite10

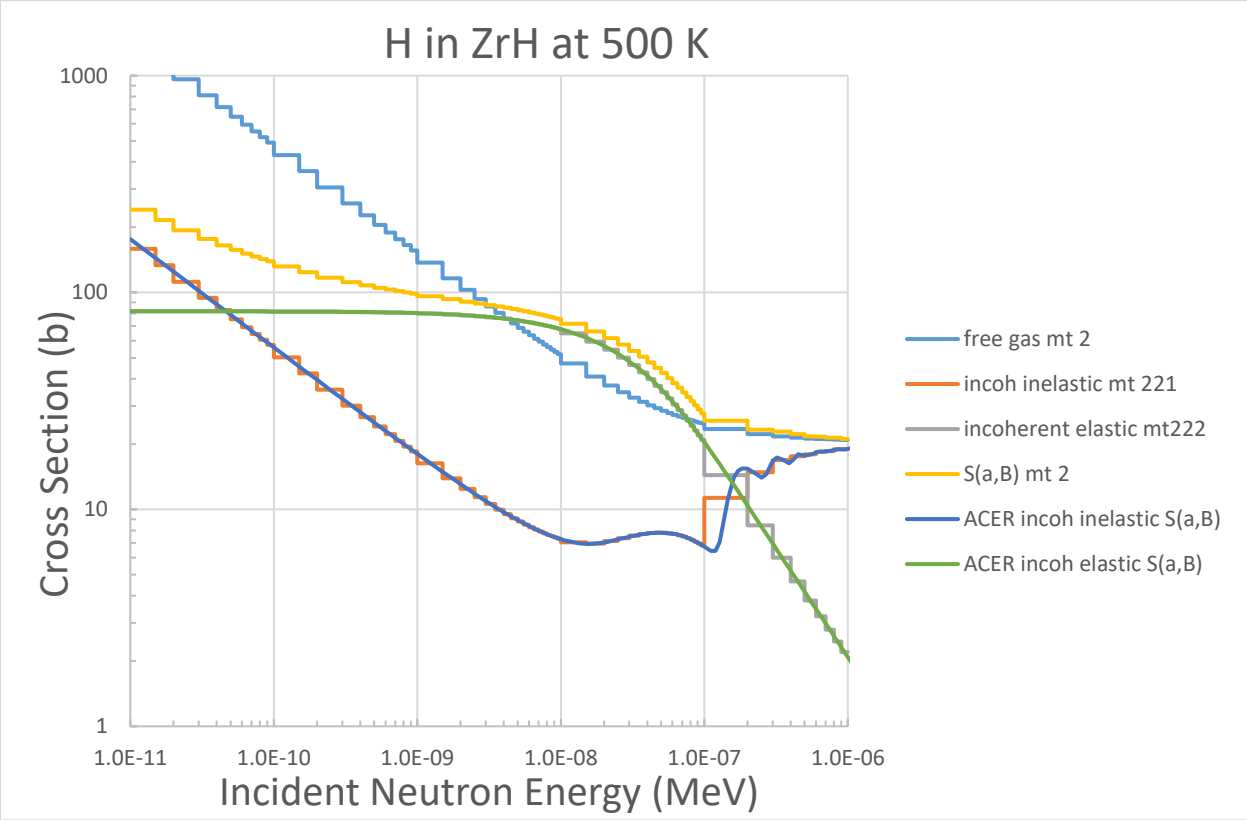

Figure 20: Comparison of ACER and GROUPR thermal scattering data for H in ZrH

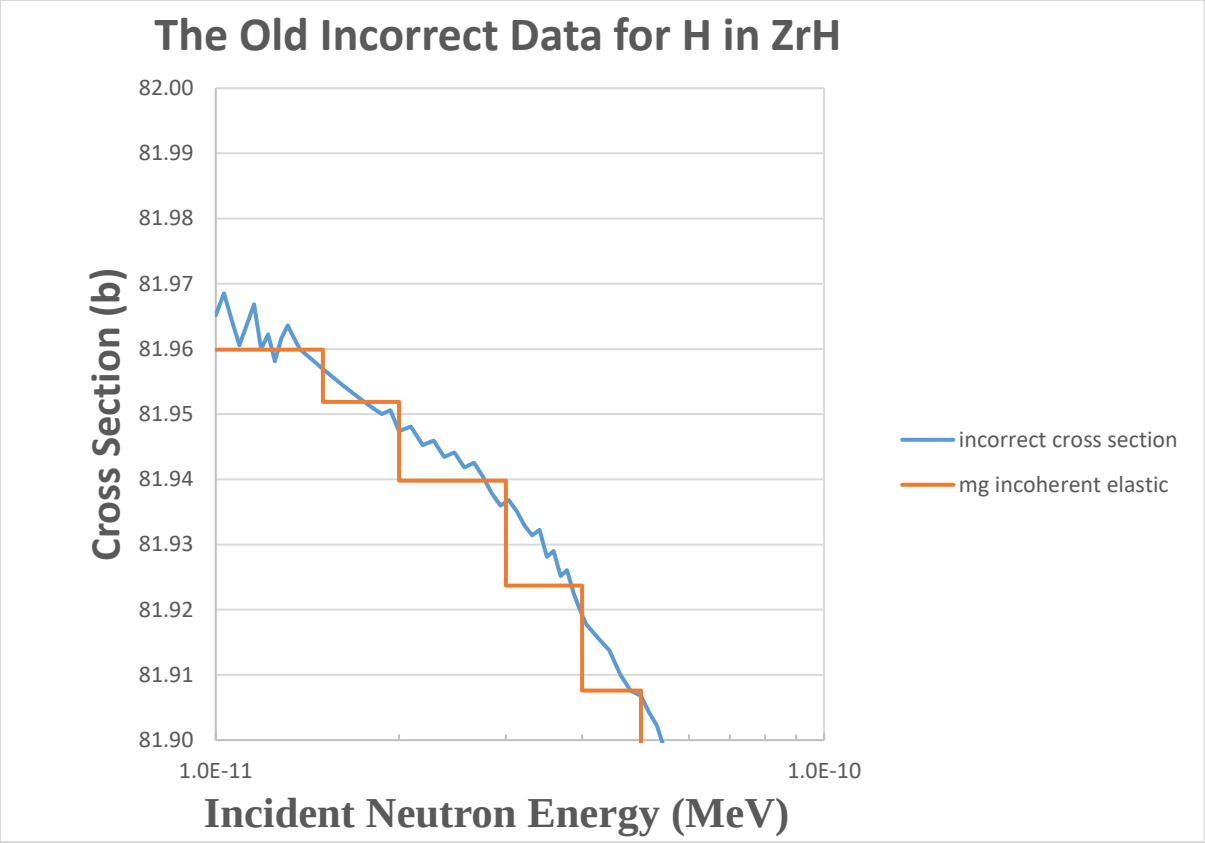

Figure 21: The Old Incorrect Data for H in ZrH and the correct GROUPR results for Incoherent Elastic Scattering

XII. Behavior of Re-Released S(α,β) Data with Temperature

For the same 3 example materials used in the ACER/GROUPR comparison, here is the ACER processed data for every temperature. In all cases, the shape of the scattering function becomes more like the free gas shape (not shown) at elevated material temperatures.

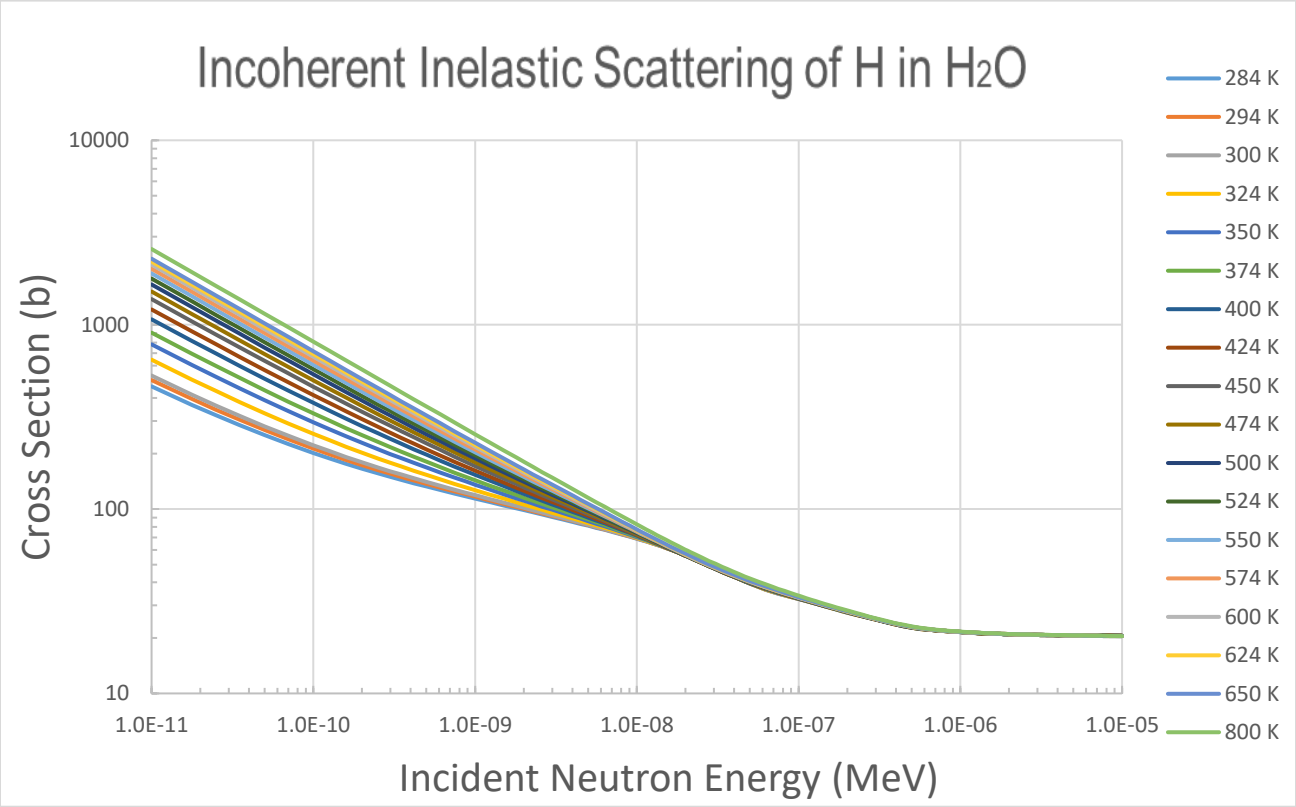

Figure 22: H Scattering in H_2O with respect to Material Temperature

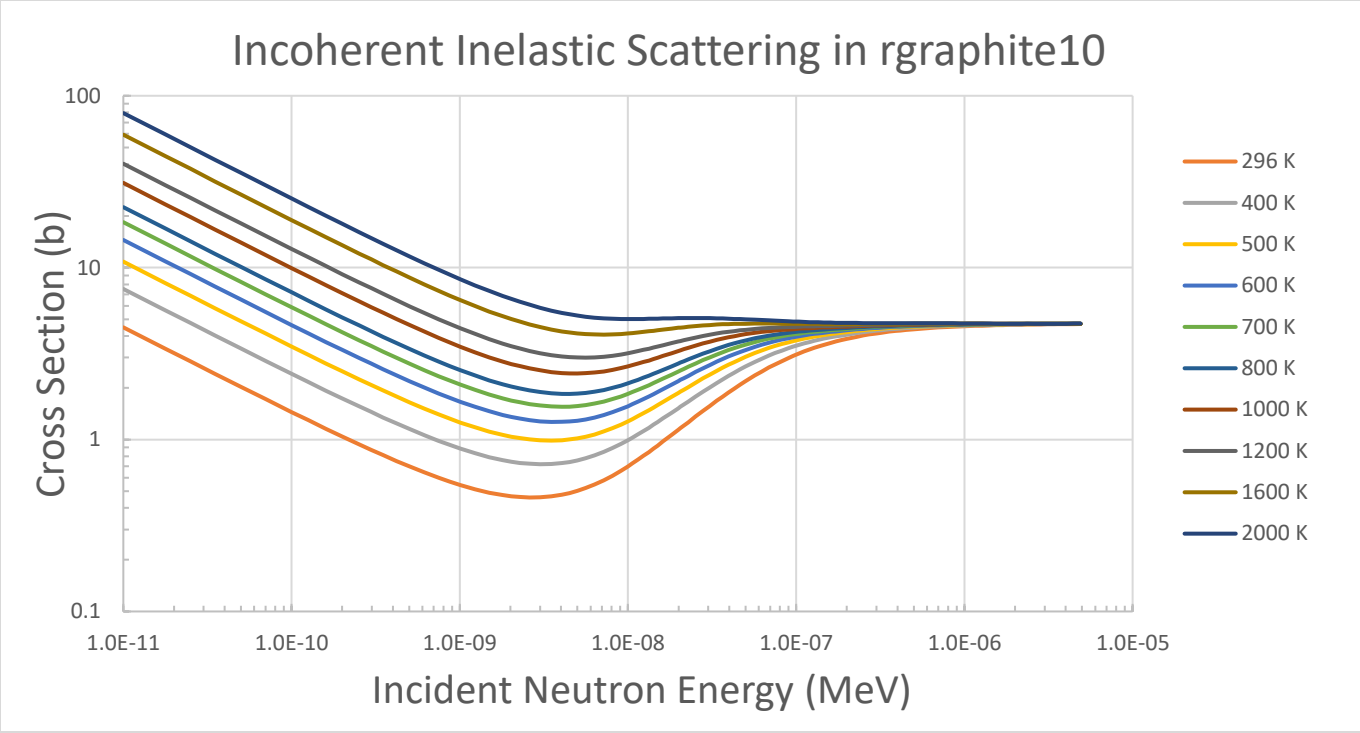

Figure 23: Incoherent Inelastic Scattering in 10% Porosity Graphite with respect to Material Temperature

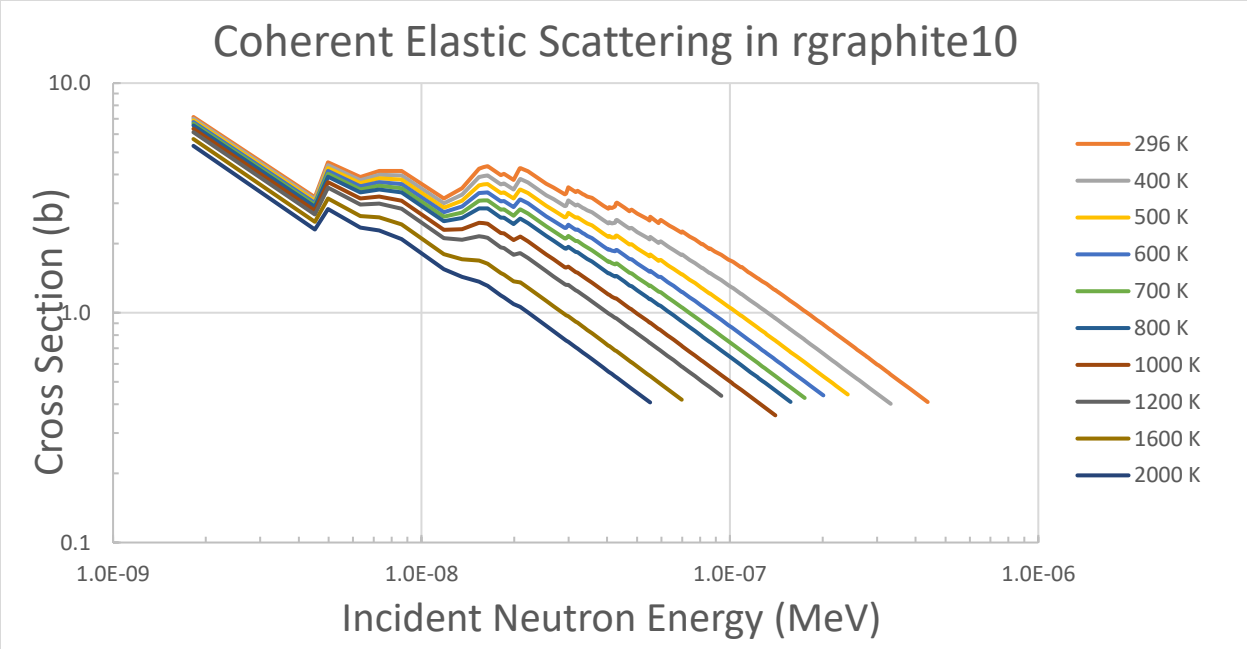

Figure 24: Coherent Elastic Scattering in 10% Porosity Graphite with respect to Material Temperature

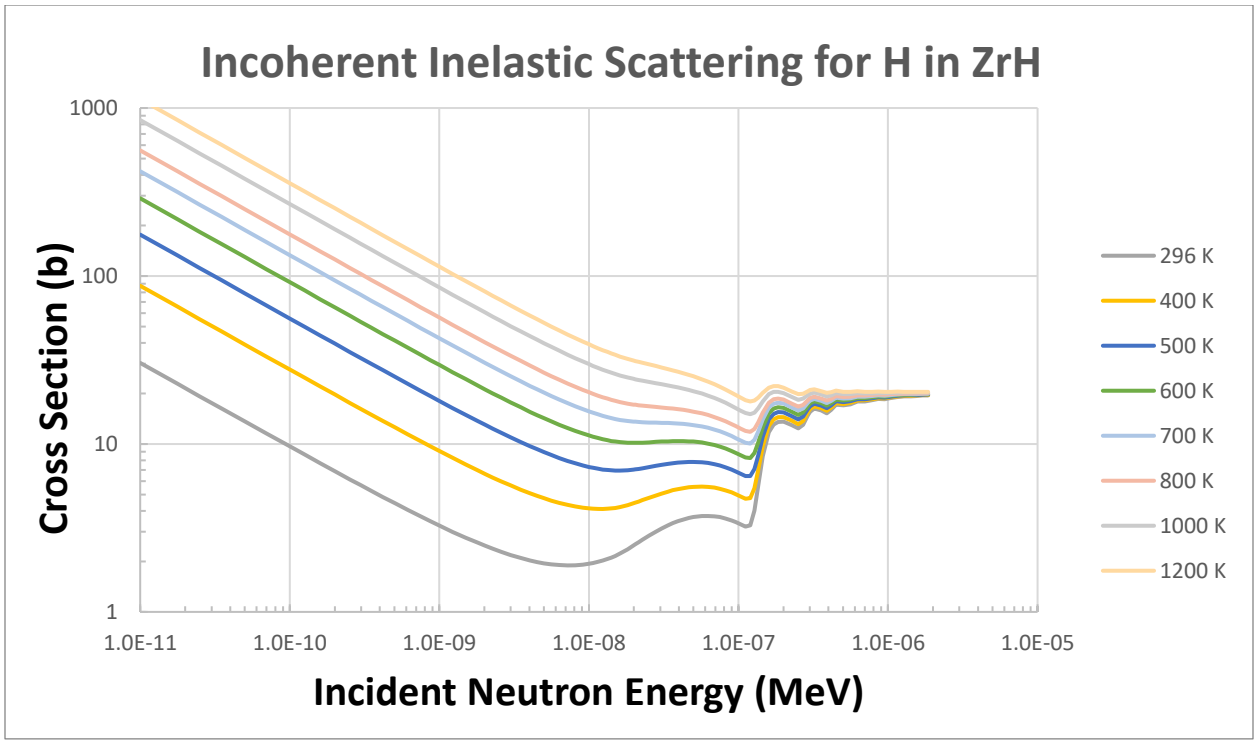

Figure 25: Incoherent Inelastic Scattering for H in ZrH with respect to Material Temperature

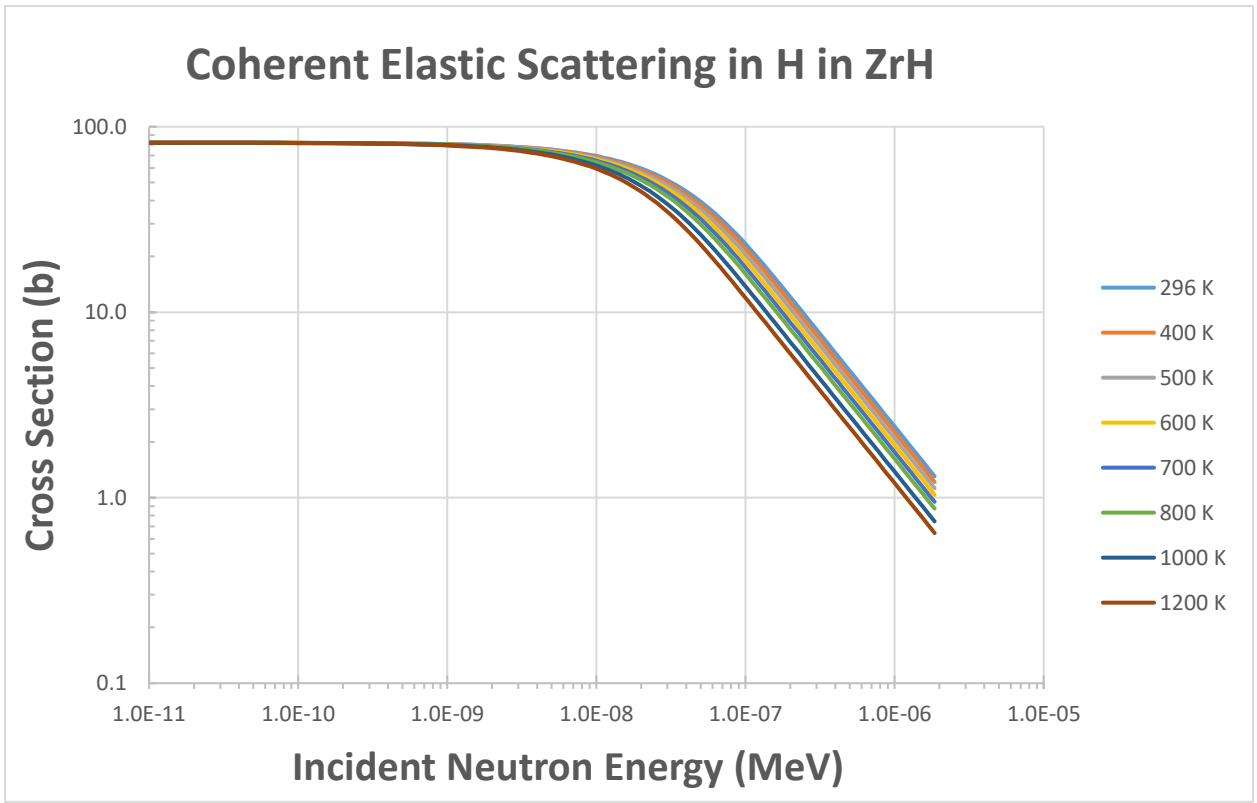

Figure 26: Coherent Elastic Scattering for H in ZrH with respect to Material Temperature

XIII. References:

1. Excerpted from David A. Brown, “README.txt” documentation file supplied with the thermal scattering data of ENDF/B-VIII.0, National Nuclear Data Center, February 2018.
2. David A. Brown, et al. "ENDF/B-VIII.0: The 8th Major Release of the Nuclear Reaction Data Library with CIELO-project Cross sections, New Standards and Thermal Scattering Data," Nuclear Data Sheets 148, 1 (2018).
3. Robert E. MacFarlane, “The NJOY Nuclear Data Processing System, Version 2016”, LA-UR-17-20093, Los Alamos National Laboratory, (2017).
4. C.J. Werner, et al., "MCNP6.2 Release Notes", Los Alamos National Laboratory, report LA-UR-18-20808 (2018).
5. D. Kent Parsons, “NJOY Processing of ENDF/B VIII.0 Thermal Scattering Files”, LA-UR-18-25096, Los Alamos National Laboratory, (2018).
6. See Table 8-4 and Equation (8-82) on p. 263 of John R. Lamarsh, *Introduction to Nuclear Reactor Theory*, Addison Wesley Publishing Company, Second Printing, September 1972.